

1 Biogeographical patterns and environmental controls of phytoplankton communities from
2 contrasting hydrographical zones of the Labrador Sea

3

4 Glauca M. Fragoso*¹, Alex J. Poulton², Igor M. Yashayaev³, Erica J. H. Head³, Mark
5 Stinchcombe², Duncan A. Purdie¹

6 1. Ocean and Earth Science, University of Southampton, National Oceanography Centre

7 Southampton, Southampton UK.; 2. Ocean Biogeochemistry and Ecosystems, National

8 Oceanography Centre; 3. Ocean and Ecosystem Science Division, Department of Fisheries

9 and Oceans, Canada, Bedford Institute of Oceanography.

10

11 *Corresponding author e-mail: (Glauca Fragoso, glauca.fragoso@noc.soton.ac.uk)

12 Permanent address: Ocean and Earth Science, National Oceanography Centre Southampton,
13 University of Southampton Waterfront Campus, European Way, Southampton SO14 3ZH,
14 United Kingdom.

15

16

17

18

19 **ABSTRACT**

20 The Labrador Sea is an important oceanic sink for atmospheric CO₂ because of intensive
21 convective mixing during winter and extensive phytoplankton blooms that occur during
22 spring and summer. Therefore, a broad-scale investigation of the responses of phytoplankton
23 community composition to environmental forcing is essential for understanding planktonic
24 food-web organization and biogeochemical functioning in the Labrador Sea. Here, we
25 investigated the phytoplankton community structure (> 4µm) from near surface blooms (< 50
26 m) from spring and early summer (2011 to 2014) in detail, including species composition and
27 environmental controls. Spring blooms (> 1.2 mg chl a m⁻³) occurred on and near the shelves
28 in May and in offshore waters of the central Labrador Sea in June due to haline- and thermal-
29 stratification, respectively. Sea ice-related (*Fragilariopsis cylindrus* and *F. oceanica*) and
30 Arctic diatoms (*Fossula arctica*, *Bacterosira bathyomphala* and *Thalassiosira hyalina*)
31 dominated the relatively cold (< 0°C) and fresh (salinity < 33) waters over the Labrador shelf
32 (e.g., on the southwestern side of the Labrador Sea), where sea-ice melt and Arctic outflow
33 predominates. On the northeastern side of the Labrador Sea, intense blooms of the colonial
34 prymnesiophyte *Phaeocystis pouchetii* and diatoms, such as *Thalassiosira nordenskiöldii*,
35 *Pseudo-nitzschia granii* and *Chaetoceros socialis*, occurred in the lower nutrient waters
36 (nitrate < 3.6 µM) of the West Greenland Current. The central Labrador Sea bloom occurred
37 later in the season (June) and was dominated by Atlantic diatoms, such as *Ephemera*
38 *planamembranacea* and *Fragilariopsis atlantica*. The data presented here demonstrate that
39 the Labrador Sea spring and early summer blooms are composed of contrasting
40 phytoplankton communities, for which taxonomic segregation appears to be controlled by the
41 physical and biogeochemical characteristics of the dominant water masses present.

43 Keywords: phytoplankton community structure; diatoms; Labrador Sea; *Phaeocystis*

44 *pouchetii*; stratification; water masses.

45

46

47

48

49

50 1. Introduction

51

52 Marine phytoplankton communities respond rapidly (days to weeks) to changes
53 occurring in their physical environment due to their short generation times. Over the last few
54 decades climate change has led to marked physical changes in the Arctic Ocean and adjacent
55 sub-Arctic seas (Yashayaev et al., 2015) – changes which are likely to be reflected by
56 responses in their phytoplankton communities (Anisimov et al., 2007). Climate-driven
57 processes modify the major factors, such as light availability, nutrient input and grazing
58 pressure that shape phytoplankton physiological traits and alter community structure
59 (Montes-Hugo et al., 2009; Litchman et al., 2012). As the climate changes in these high
60 latitude oceans, the parameters that define the phytoplankton phenology (seasonal and
61 interannual variation), biomass, primary production and community structure, will all likely
62 be modified. Alteration of the phytoplankton community propagates into marine food web
63 dynamics and biogeochemical cycles (Finkel et al., 2010), due to traits regarding palatability,
64 cell size, elemental stoichiometry and efficiency of carbon transport to deeper waters. A
65 further advance in understanding the long-term responses of Arctic phytoplankton to climate
66 change can be achieved from remote-sensing-derived observations (e.g., Arrigo et al., 2008;
67 Pabi et al., 2008; Kahru et al., 2011; Ardyna et al., 2014) and *in situ* long-term monitoring
68 (Head et al., 2003; Yashayaev, 2007; Yashayaev et al., 2015).

69 The Labrador Sea is a sub-Arctic region of the Northwest Atlantic located between
70 Greenland and the eastern coast of Canada. In spite of its small size (< 1% of the Atlantic
71 Ocean), the Labrador Sea plays a critical role in the marine carbon cycle because it is one of
72 the most productive regions of the North Atlantic, which enhances the flux of atmospheric
73 CO₂ into surface waters (DeGrandpre et al., 2006; Martz et al., 2009). Moreover, the

74 Labrador Sea produces the densest of all water masses that are entirely formed in the
75 subpolar North Atlantic (Yashayaev et al., 2015), where wintertime cooling and wind forcing
76 cause convective sinking of dense surface water, transporting carbon rapidly to the deep
77 ocean (Tian et al., 2004). The Labrador Sea is also a region susceptible to climate change
78 because it receives the discharge of Arctic ice-melt waters, which potentially increases the
79 freshening of surface layers (Dickson et al., 2002; Yashayaev and Seidov, 2015). Due to its
80 biogeochemical significance and potential vulnerability to climate change, a comprehensive
81 understanding of the current phytoplankton communities in the Labrador Sea is crucial to
82 detect climate change effects in the future.

83 The Labrador Sea is usually characterised by three distinct phytoplankton bloom
84 regions during spring and early summer (Frajka-Williams et al., 2009, Frajka-Williams and
85 Rhines, 2010). In contrast to the south to north progression observed in other regions of the
86 North Atlantic (Henson et al., 2009), the northern bloom (north of 60°N, in the eastern
87 Labrador Sea) is more intense (satellite-derived chlorophyll (1998-2006) up to 5.5 mg chl *a*
88 m⁻³, Harrison et al., 2013) and starts early in the season (late April). This is due to the early
89 onset of haline-driven stratification formed by freshwater input from the West Greenland
90 Current (Stuart et al., 2000; Frajka-Williams and Rhines, 2010; Harrison et al., 2013; Lacour
91 et al., 2015). The western bloom located on the Labrador Shelf varies inter-annually, since it
92 is triggered by the rapid melting of sea ice that often covers the shelf well into spring (Wu et
93 al., 2007). The Labrador Shelf bloom development starts as the ice retreats, which is usually
94 in May, although it may occur later (June) in some years (Head et al., 2013). The central
95 Labrador bloom is weaker (1998-2006 satellite-derived chlorophyll < 2 mg chl *a* m⁻³,
96 Harrison et al., 2013) and occurs later in the season (June) as a result of thermal stratification
97 (Frajka-Williams and Rhines, 2010). Nutrient replenishment, occurring during deep winter
98 mixing (200 – 2300 m) and dependent on cumulative surface heat loss, (Yashayaev and

99 Loder, 2009), supports the phytoplankton spring bloom once light becomes available
100 (Harrison et al., 2013). Storm events (Wu et al., 2008) as well as upwelling events from
101 cyclonic eddies (Yebra et al., 2009) and glacial meltwater (Bhatia et al., 2013) have all been
102 suggested to sustain the blooms via nutrient replenishment after these are exhausted in
103 surface waters.

104 The Labrador Sea acts as a receiving and blending basin for Atlantic and Arctic
105 waters (Yashayaev et al., 2015) and, therefore, is an ideal region to study the influence of the
106 environmental factors that shape the phytoplankton community structure due to the Atlantic
107 and Arctic waters that divide the region into distinct hydrographic zones (Head et al., 2000,
108 2003). Hydrographic zones create ecological niches, where distinct phytoplankton
109 communities occur (Acevedo-Trejos et al., 2013; Goes et al., 2014, Brun et al., 2015).
110 Understanding the drivers of biogeographical patterns of phytoplankton communities in the
111 Labrador Sea will provide insights about the habitat complexity of this area, in addition to
112 elucidating the phytoplankton responses to future changes. Plankton community structure
113 from the Labrador Sea has previously been assessed by bio-optical, pigment or microscopic
114 observations (Head et al., 2000; Stuart et al., 2000; Cota et al., 2003; Strutton et al., 2011;
115 Harrison et al., 2013). Nonetheless, a detailed quantitative taxonomic analysis of the
116 environmental controls on phytoplankton communities and species composition has not
117 previously been carried out.

118 Based on *in situ* observations collected in the Labrador Sea during late spring and
119 early summer (2011 – 2014), the specific goals of this study were:

120 1) to describe the biogeographical patterns of spring phytoplankton communities across the
121 Labrador Sea,

122 2) to investigate the major hydrographic parameters that influence taxonomic segregation of
123 phytoplankton blooms from the upper 50 m in the Labrador Sea,
124 3) to discuss the major environmental drivers for specific phytoplankton groups (e.g.
125 *Phaeocystis pouchetii* and diatoms) in this high latitude sea.
126

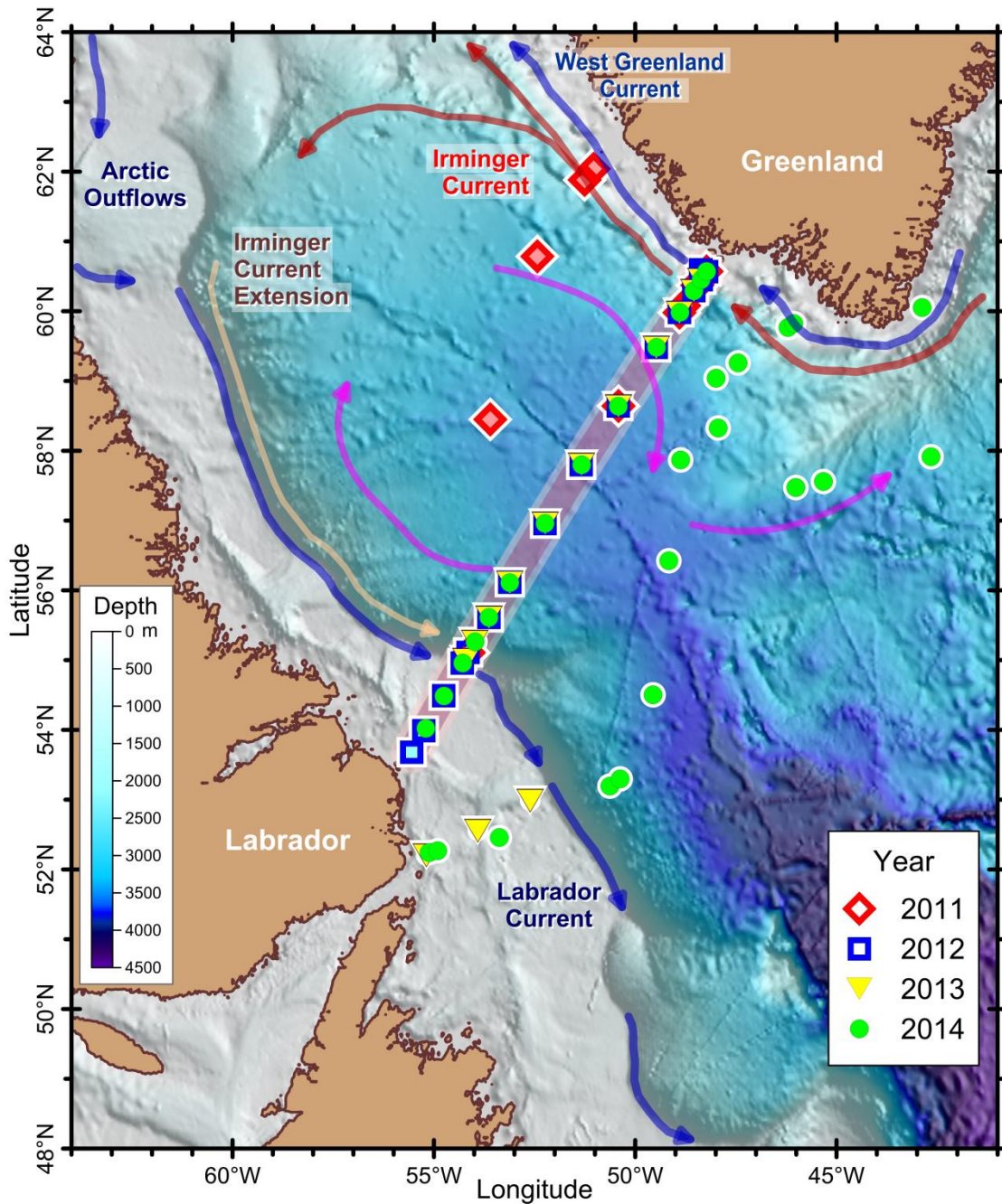
127 **2. Methods**

128 *2.1 Study area*

129 The Labrador Sea and the entire subpolar North Atlantic receive buoyant fresh and
130 cold Arctic outflow (Yashayaev et al., 2015) through two major pathways. One of these
131 pathways connecting the Labrador Sea to the Arctic Ocean originates from the Baffin Island
132 Current that crosses Davis Strait and subsequently merges with various southward inshore
133 flows to become the Labrador Current (LC) (Fig. 1). The other pathway starts with the East
134 Greenland Current (EGC) in the Greenland Sea (Yashayaev and Seidov, 2015), which turns
135 around the southern tip of Greenland and flows northwards along the Greenland coast to
136 become the West Greenland Current (WGC)(Yashayaev, 2007) (Fig. 1). The LC is composed
137 of two main branches: an inshore branch, which occupies the Labrador Shelf, and an offshore
138 branch, which is centred over the 1000 m contour. The inshore branch receives waters of
139 Arctic origin via Davis and Hudson Straits, whereas the offshore branch receives
140 contributions from the outflow from Davis Strait and from the portion of the WGC that turns
141 west and then south along the shelf-break (Head et al., 2013) (Fig. 1). The inflow from
142 Hudson Strait contains a large riverine input from Hudson Bay, increasing the contribution of
143 estuarine waters to this water mass (15% of total volume of the LC) (Straneo and Saucier,
144 2008). Local ice melting also influences the properties of the LC, given that the Labrador
145 Shelf is a seasonal ice zone, where sea ice starts forming in mid-January, reaching its
146 maximum at the end of March and starts to melt in May (Wu et al., 2007).

147 The shallow fresh and cold WGC presents a mixture of low salinity Arctic water from
148 the EGC and Greenland ice melt (collectively sourced from glaciers, icebergs and Greenland
149 ice surface melts). The WGC is also influenced by the relatively warm and saline Atlantic
150 water, which, in turn, originates from the Irminger Current (IC) (Yashayaev, 2007, 2015)
151 (Fig. 1). Sea ice is prevented from forming on the Greenland Shelf, although icebergs are
152 frequent (De Sève, 1999; Yankovsky and Yashayaev, 2014). The deep central basin (water
153 depths from 3200 to 3700 m) of the Labrador Sea features a clockwise (anticyclonic)
154 circulation, which in turn contributes to an anticlockwise (cyclonic) gyre nested along the
155 outer rim of the deep basin (Yashayaev, 2007; Hall et al., 2013; Kieke and Yashayaev, 2015)
156 (Fig. 1).

157 The Labrador Sea is a region with complex, yet, well-structured hydrography
158 characterised by marked fronts maintained by the major currents such as the LC, IC and
159 WGC. These oceanographic fronts separate characteristic zones composed of distinct water
160 masses (Yashayaev, 2007). Boundary currents are concentrated at the Greenland and
161 Labrador slopes, where anticyclonic/cyclonic mesoscale eddies are common, particularly
162 Irminger Rings, located in the eastern part of the Labrador Sea (Frajka-Williams et al., 2009;
163 Yebra et al., 2009).



164

165 Figure 1. Map showing the stations and currents of the Labrador Sea. Stations were sampled along the
 166 AR7W transect (background line) during multiple years (2011 - 2014) or near the transect in 2011
 167 (red diamonds), 2012 (blue squares), 2013 (inverted triangles), and 2014 (green dots). Scale refers to
 168 bathymetry. Circulation elements - colder currents (Labrador Current, Arctic Outflows and West
 169 Greenland Current, blue solid arrows), warmer currents (Irminger Current and Extension, red and
 170 brown solid arrows, respectively) and the anticyclonic circulation gyre (pink solid arrows) of the
 171 Labrador Sea.

172

173 *2.2 Sampling*

174

175 Initiated as a part of the *World Ocean Circulation Experiment* (WOCE), and then
176 included as a key component into the *Climate and Ocean: Variability, Predictability and*
177 *Change* (CLIVAR) sampling plan, the oceanographic section AR7W (following WOCE
178 terminology) running across the Labrador Sea has been occupied annually by the *Ocean and*
179 *Ecosystem Science Division* of the *Bedford Institute of Oceanography* (BIO) since 1990. This
180 sustained full-depth sampling and monitoring of one of the most critical ocean basins
181 includes collection and analysis of a broad variety of physical, chemical, and biological
182 observations across the Labrador Sea and has recently been established as the principal
183 component of the *Atlantic Zone Off-Shelf Monitoring Program* (AZOMP) of the *Department*
184 *of Fisheries and Oceans Canada*. This section line, still commonly referred to as AR7W,
185 extends from Misery Point just inshore of the Hamilton Bank on the Labrador Shelf to Cape
186 Desolation on the Greenland Shelf (Fig. 1). The transect has 28 fixed position hydrographic
187 stations when ice conditions do not prevent sampling on either of the shelves, in addition to
188 some extra stations that are sampled, which vary annually.

189 Data for this study were collected on five research cruises (HUD-2011-009, HUD-
190 2012-001, HUD-2013-008, HUD-2014-007, and JR302) to the Labrador Sea. The dates of the
191 respective expeditions carried out by the *CCGS Hudson* (HUD-Year-ID) were May 11 - 17,
192 2011, 4 - 12 June, 2012, 9 - 21 May, 2013, and 7 - 14 May, 2014, and by the *RRS James*
193 *Clark Ross* (JR302) – June 10 - 24, 2014. Stations were sampled on two transect crossings of
194 the shelves and deep basin of the Labrador Sea (Fig. 1). The AR7W line was sampled
195 annually on the *Hudson* with additional stations sampled south of the AR7W line in June
196 2014 on the JR302 cruise. In addition to these two transects, occasional other stations were
197 also sampled in the Labrador Sea (Fig. 1).

198 Vertical continuous profiles of temperature, salinity and chlorophyll fluorescence
199 were measured with a CTD/rosette system. Water samples were collected on the upward

200 CTD casts using 10-L Niskin bottles mounted on a rosette frame. Mixed layer depths were
201 calculated from the vertical density (σ_θ) distribution and defined as the depth where σ_θ
202 changes by 0.03 kg m^{-3} from a stable surface value ($\sim 10 \text{ m}$) (Weller and Plueddemann, 1996).
203 As this mixed layer depth criterion presents limitations in accurately identifying weakly
204 versus strongly stratified water masses, an additional and more robust criterion was used to
205 measure stratification – a stratification index (SI). In this study, the SI was calculated as the
206 difference in σ_θ values between 60m and 10 m divided by the respective difference in depth
207 (50 m).

208 For phytoplankton biomass determination from near surface waters of the Labrador
209 Sea, mixed water samples from the upper 50 m (i.e. a mixture of 50 mL from each of 6
210 depths: 0, 10, 20, 30, 40, and 50m – (see Figure 9) and from the surface ($<10 \text{ m}$) in case of
211 samples from early summer 2014 (JR302 cruise) were collected and immediately preserved
212 in acidic Lugol's solution to a final concentration of 2%. Samples were stored in dark glass
213 bottles for later phytoplankton species identification and enumeration in the laboratory.
214 Discrete water samples were collected for chlorophyll *a* (chl*a*) and nutrient analysis between
215 the surface to a depth of 100 m at every 10 m or 25 m intervals (for more details, see Figure
216 9, supplemental material). Samples for nutrient analysis were frozen at -20°C and measured
217 using an autoanalyzer (Alpkem RFA-300) or manually (ammonium, NH_4^+) using the
218 hypochlorite method of Solórzano (1969) or the fluorometric method of Kerouel and Aminot
219 (1997) (JR302 cruise). Chlorophyll *a* was extracted in 90% acetone for approximately 24
220 hours at -20°C and fluorometrically determined using a Turner Designs fluorometer (Holm-
221 Hansen et al., 1965). Samples for particulate organic carbon (POC) were filtered (0.25 L –
222 1L) onto 25 mm pre-combusted GF/F filters and rinsed with 0.01 N HCl filtered seawater to
223 remove inorganic carbonates and oven-dried (60°C) for 8-12 hours. Samples were kept dry

224 and analysed in the laboratory using a Carbon-Hydrogen-Nitrogen (CHN) analyser (Collos,
225 2002).

226

227

228 2.3 Phytoplankton enumeration

229

230 Lugols preserved samples were counted to determine phytoplankton ($> 4 \mu\text{m}$)
231 abundance and taxonomic composition. According to cell abundance (previously observed
232 under the light microscope), 10 or 25-ml of each sample was placed in settling chambers for
233 24 h and examined using a Leiss inverted microscope under x100 or x200 magnification
234 (Utermöhl, 1958). Large ($> 50 \mu\text{m}$) and numerically rare taxa were counted during full
235 examination of the settling chamber at x100 magnification, while small ($< 50 \mu\text{m}$) and
236 numerically dominant taxa were counted on 1 or 2 transects of the chamber at x200
237 magnification. At some stations where large taxa were dominant, such as the diatoms
238 *Ephemera planamembranaceae* and *Thalassiosira* spp., at least 300 individuals were counted
239 in 1 or 2 transects at x100 magnification. Counting units were considered as individuals cells,
240 regardless of whether they were solitary or in a chain/colony, except for *Phaeocystis*
241 *pouchetii* colonies, which were considered individuals categorized by colony size (small:
242 $<100 \mu\text{m}$, medium: $100 - 199 \mu\text{m}$, large: $200 - 299 \mu\text{m}$ and extra large $> 300 \mu\text{m}$). Cell
243 abundance within each size category of colony was estimated as the average number of cells
244 counted in at least 10 different colonies of that size category. *P. pouchetii* single cells, either -
245 flagellated or derived from colonies, were counted and grouped together.

246 Diatoms and dinoflagellates were identified to genus or species whenever possible
247 following Medlin and Priddle (1990), Tomas (1997) and Thronsen et al. (2007).
248 Unidentified dinoflagellate taxa were grouped as small ($4 - 29 \mu\text{m}$) or large ($>30 \mu\text{m}$), and

249 with reference to cell wall structure (naked or armored). Unidentified diatoms were grouped
250 as centric or pennate according to a size category (i.e. 4 - 19 μm , 20 - 49 μm , 50 - 99 μm , 100
251 - 149 μm , 150 - 200 μm and $>200 \mu\text{m}$). *Thalassiosira* and *Fragilariopsis* species
252 identification were only possible using a Scanning Electron Microscope (SEM), except for
253 *Fragilariopsis atlantica*, and therefore *Fragilariopsis* genus were also categorized by size:
254 small (4 - 19 μm), medium (20 - 50 μm) and large ($>50 \mu\text{m}$). The genus *Chaetoceros* was
255 also classified by size as large (subgenus *Phaeoceros*), medium (*C. decipiens*, *C. mitra*, *C.*
256 *lacinosus*, *C. debilis*, *C. curvisetus*) or small (*C. compressum*, *C. socialis* and others which
257 could not be identified to species level using the light microscope). It was not possible to
258 identify most of the nanoflagellates, other than cryptophytes, *P. pouchetii* and small
259 dinoflagellates, and therefore unidentified flagellates are not included in this study (median
260 and standard error biomass = $12 \pm 3\%$ of total biomass).

261

262 2.4 Biovolume and biomass estimation

263

264 Cell biovolume was calculated based on geometrical shapes assigned for each taxa as
265 suggested by Sun and Liu (2003). Cell dimensions of at least 10 specimens were measured
266 and biovolume for each taxon was compared to the literature (Olenina et al., 2006). Cell
267 carbon concentrations were estimated using carbon conversion factors for diatoms
268 (Montagnes and Franklin, 2001) and other protists (Menden-Deuer and Lessard, 2000). For
269 *P. pouchetii*, total carbon biomass consisted of cell biomass (either -flagellated, non-motile or
270 colony-bound cells) and biomass contained in the mucus of *Phaeocystis* colonies. *P.*
271 *pouchetii* cell carbon biomass was estimated based on geometrical shape as previously
272 described, without any distinction between flagellate, non-motile or colony-bound cells. A
273 mucus carbon conversion factor has previously been developed to convert from colony

274 volume to total colony biomass for *P. antarctica* (213 ng C mm⁻³, Mathot et al., 2000) and *P.*
275 *globosa* (335 ng C mm⁻³, Rousseau et al., 1990). Given the lack of data on carbon estimates
276 of colonial mucus for *P. pouchetii*, the average colonial mucus reported from *P. antarctica*
277 and *P. globosa* was applied for *P. pouchetii* colonies in this study (i.e. 274 ng C mm⁻³). A
278 regression analysis ($y = 1.01x + 240.92$; $r^2 = 0.47$; $n = 44$; $p < 0.0001$) of the carbon
279 calculated from cell counts and carbon derived from POC analysis showed good agreement.
280 The goodness-of-fit was confirmed by visually observing the normal distribution of the
281 residuals.

282

283 *2.5 Statistical analyses*

284

285 Phytoplankton community structure in the Labrador Sea during late spring and early
286 summer of 2011 - 14 was investigated using PRIMER-E (v7) software (Clarke and Warwick,
287 2001). Biomass data from the 75 phytoplankton taxa (including species, genus and different
288 morphotypes) were normalized by performing a square root transformation, allowing each
289 taxon to influence the similarity within and among samples. Bray-Curtis similarity was
290 calculated within each pair of samples and a Cluster analysis of this matrix was generated to
291 display the similarity relationship among samples. An arbitrary threshold (46% of similarity)
292 was applied to link the samples that are more similar to each other (i.e. > 46% similar in
293 terms of taxa composition) into Cluster groups.

294 A non-metric multi-dimensional scaling (nMDS) plot was used to visually display the
295 similarity relationship between the respective pairs of samples derived from Bray-Curtis
296 similarity matrix. Thus, samples that reflected greater community resemblances were
297 spatially closer than the ones that were less similar. The stress level of the nMDS plot is a
298 measurement of how accurate the representation is, with lower stress values being associated

299 with better visual representation of the similarity relationship in 2-D space. Bubble plots were
300 constructed in the nMDS plots to identify the associations between blooms (in terms of
301 carbon biomass and chl a) and physical parameters (MLD and SI). For this analysis, a
302 threshold of median chlorophyll a biomass values greater than 1.2 mg chl a m $^{-3}$ for each
303 Cluster was applied to arbitrarily define bloom conditions at the upper 50 m.

304 The similarity percentage analysis (SIMPER) routine was used to explore the
305 dissimilarities between Clusters and the similarities within Clusters of samples. Moreover,
306 this output was used to identify the contributions from each taxon to the (average) overall
307 similarity within Clusters at a cutoff of 90% cumulative contribution. A post-hoc analysis of
308 similarity (one-way ANOSIM) was also applied to determine whether Clusters were
309 statistically significantly different from each other in terms of their taxonomic composition.

310 To analyse the effects of gradients (environmental parameters) on the Labrador Sea
311 phytoplankton biomass and community structure, a redundancy analysis (RDA) was
312 performed using the CANOCO 4.5 software (CANOCO, Microcomputer Power, Ithaca, NY).
313 This multivariate analysis determines the environmental variables (explanatory variables) that
314 best explain the distribution of the major selected taxa, by selecting the linear combination of
315 environmental variables that yields the smallest total residual sum of squares in the
316 taxonomic data (Peterson et al., 2007). Only taxa that contributed to more than 0.5% of total
317 biomass (reduced from 75 to 11 taxa) were selected for RDA analysis. Detrending canonical
318 correspondence analysis (DCCA) was used *a priori* to determine whether the data ordination
319 method was linear (suitable for RDA analysis) or unimodal (suitable for Canonical
320 Correspondence Analysis – CCA). A relatively small gradient length (< 2.5 standard
321 deviation units according to DCCA analysis output) revealed that the ordination was linear-
322 based and that RDA analysis was suitable (Lepš and Šmilauer, 2003). Forward-selection (*a*
323 *posteriori* analysis) was used to identify a subset of environmental variables that significantly

324 explained taxonomic distribution and community structure when analysed individually (λ_1 ,
325 marginal effects) or included in the model where other forward-selected variables were
326 analysed together (λ_a , conditional effects). Biomass data were log-transformed and a Monte
327 Carlo permutation test ($n = 999$, reduced model) was applied to test the statistical significance
328 ($p < 0.05$) of each of the forward-selected variables.

329

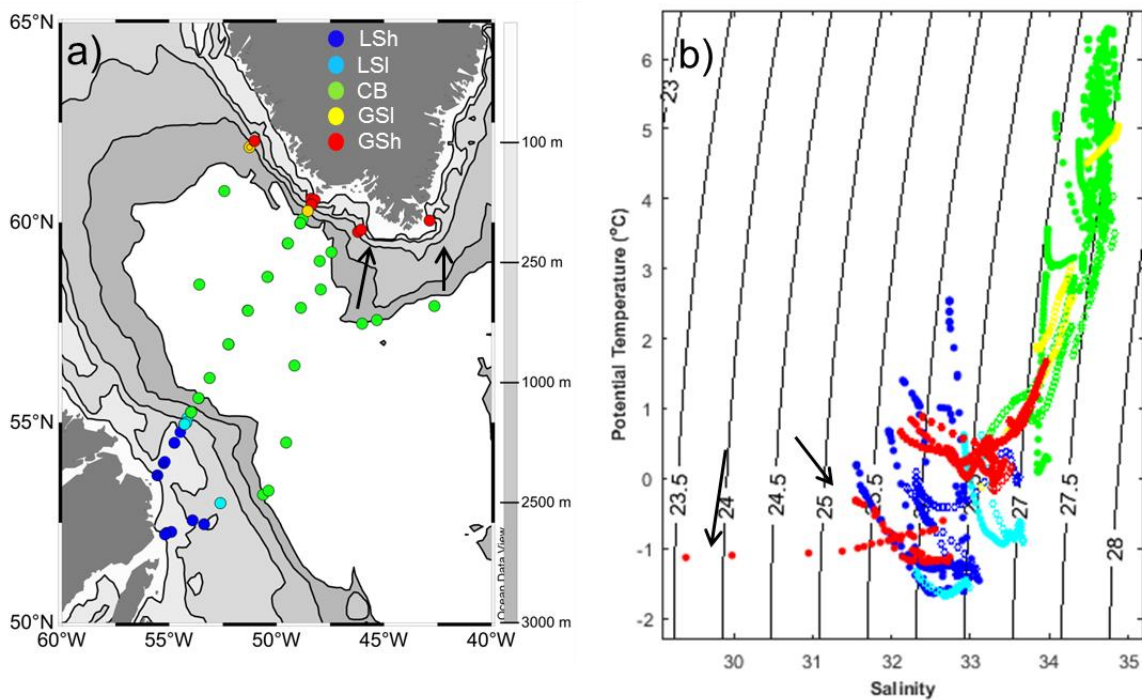
330 **3. Results**

331 *3.1 Hydrography and nutrient distributions*

332 The Labrador Sea was divided into five distinct zones based on its bathymetry – a
333 wide and shallow shelf (< 250 m) and slope (250 m – 1000 m) located close to Canada
334 (Labrador Margin), a deep central Basin (> 2500 m) and a narrow and steep slope (2500 m –
335 3000 m) and shelf (< 2500 m) on the Greenland Margin (Fig. 2a). Temperature and salinity
336 from surface and sub-surface waters (upper 50 m) varied among these distinct zones across
337 the Labrador Sea (Fig. 2b). In general, colder (temperature $< 2^\circ\text{C}$), fresher (salinity < 34) and
338 less dense waters ($\sigma_\theta < 27 \text{ kg m}^{-3}$) were found on the shelves and slope regions (Fig. 2b),
339 particularly on the Labrador Shelf and Slope and at the Greenland Shelf during late June (see
340 the arrows in Fig. 2a and b), indicating the influence from the Arctic outflow. A warmer
341 (temperature $> 1^\circ\text{C}$), saltier (salinity > 33.5) and denser ($\sigma_\theta > 27 \text{ kg.m}^{-3}$) water mass with
342 features of modified Atlantic waters (Irminger Current, IC) was found widely distributed in
343 the central portion and Greenland slope of the Labrador Sea (Fig. 2). The temperature and
344 salinity (T-S) properties from the surface and subsurface waters varied interannually (2011 -
345 2014) and seasonally (from early May until late June) during the period of study (Fig. 2b).

346 In spite of the interannual variability, the T-S properties of the surface/subsurface
347 waters of most stations on the Labrador Shelf were generally colder and fresher (average T =

348 -0.6°C and salinity = 32.6) than the waters on the Greenland Shelf (average T = 0.3°C and
 349 salinity = 33.1) during May, suggesting that the former was influenced by direct inputs of
 350 fresher and colder water from the Arctic, Hudson Bay, continental run-off and from local sea-
 351 ice melt (Fig. 2b). However, instances of extremely fresh and cold waters were also found in
 352 late June 2014 at some stations south of Greenland, suggesting the influence of additional
 353 glacial melt in this region (Fig. 2b, see arrows). The positions of fronts, usually recognised by
 354 a sharp gradient between Arctic and modified Atlantic (Subpolar Mode and IC) waters,
 355 varied from year to year, but were generally located near the continental slopes (data not
 356 shown).

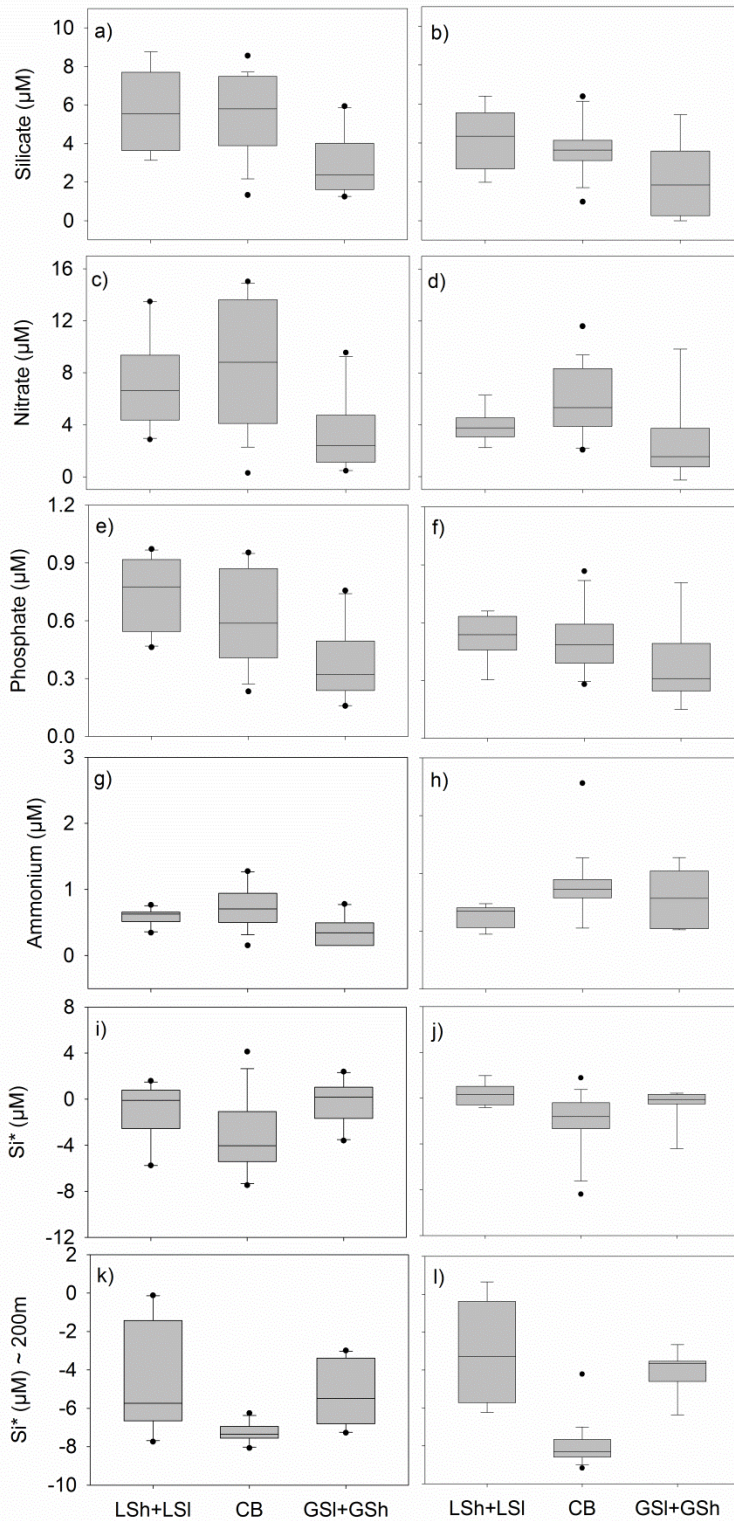


357
 358 Figure 2. Biogeographical zones in the Labrador Sea classified by bathymetry: (a) Labrador Shelf
 359 (LSh), Labrador Slope (LSI), Central Basin (CB), Greenland Shelf (GSh) and Greenland Slope (GSI);
 360 and (b) potential temperature and salinity (T-S) with isopycnals (σ_θ) scatter plot of the upper 50 m
 361 waters from these five zones during May (open circles) and June (closed circles) of 2011 -2014.
 362 Arrows indicate the stations on the Greenland Shelf and the corresponding T-S signature during late
 363 June 2014.

364 Nutrient concentrations from the surface and subsurface waters (upper 50 m) varied
 365 spatially and temporally across the Labrador Sea (Fig. 3). In general, the temporal variation

366 in nutrient concentrations (nitrate, silicate, phosphate and Si* (silicate minus nitrate
367 concentration)) had similar trends during May and June (Fig. 3a-f, 3i-l), except ammonium
368 concentrations, which were clearly higher in the Central Basin and Greenland Shelf and
369 Slope (median > 0.8 μM) during June (Fig. 3g,h). In general, nitrate, silicate and phosphate
370 concentrations were lowest on the Greenland Shelf and Slope (Fig. 3a-f). Median nitrate
371 concentrations were clearly higher in the Central Basin (> 8 μM in May and > 5 μM in June),
372 (Fig. 3c,d). Median silicate concentrations were greater in the central western part of the
373 Labrador Sea (Labrador Shelf and Slope, and Central Basin), where median concentrations
374 were > 5 μM in May and > 4 μM in June (Fig. 3a,b). Phosphate concentration was higher in
375 the western part of the Labrador Sea, on the Labrador Shelf and Slope (median > 0.8 μM in
376 May and > 0.5 μM in June) and decreased eastwards (Fig. 3e,f).

377 The central Basin had median Si* < 0 μM , which suggests that the phytoplankton
378 from these regions experienced, in most cases, an excess of nitrate compared to silicate
379 (median Si* = -4 μM during May and -1 μM during June, respectively), although there were
380 some stations in the central Basin region where Si* values were > 0 μM (Si* up to 4 μM)
381 (Fig. 3i,j). The Labrador Shelf had higher median Si*, particularly during June (Si* up to 1
382 μM) (Fig. 3j) and the Greenland Shelf had Si* values approaching zero (Fig. 3i,j). The
383 Labrador Shelf also had higher Si* values at depth (Si* from -6 μM up to -1 μM
384 approximately at 200 m or the deepest depth if bottom depth is < 200 m) compared to the
385 other regions (Si* < -4 μM), although in general, these waters had an excess of nitrate
386 compared to silicate (i.e. negative values, Fig. 3k,l). Higher Si* in shelf waters, particularly
387 on the Labrador Shelf, may be associated with input of riverine and glacial meltwaters
388 enriched with silica.



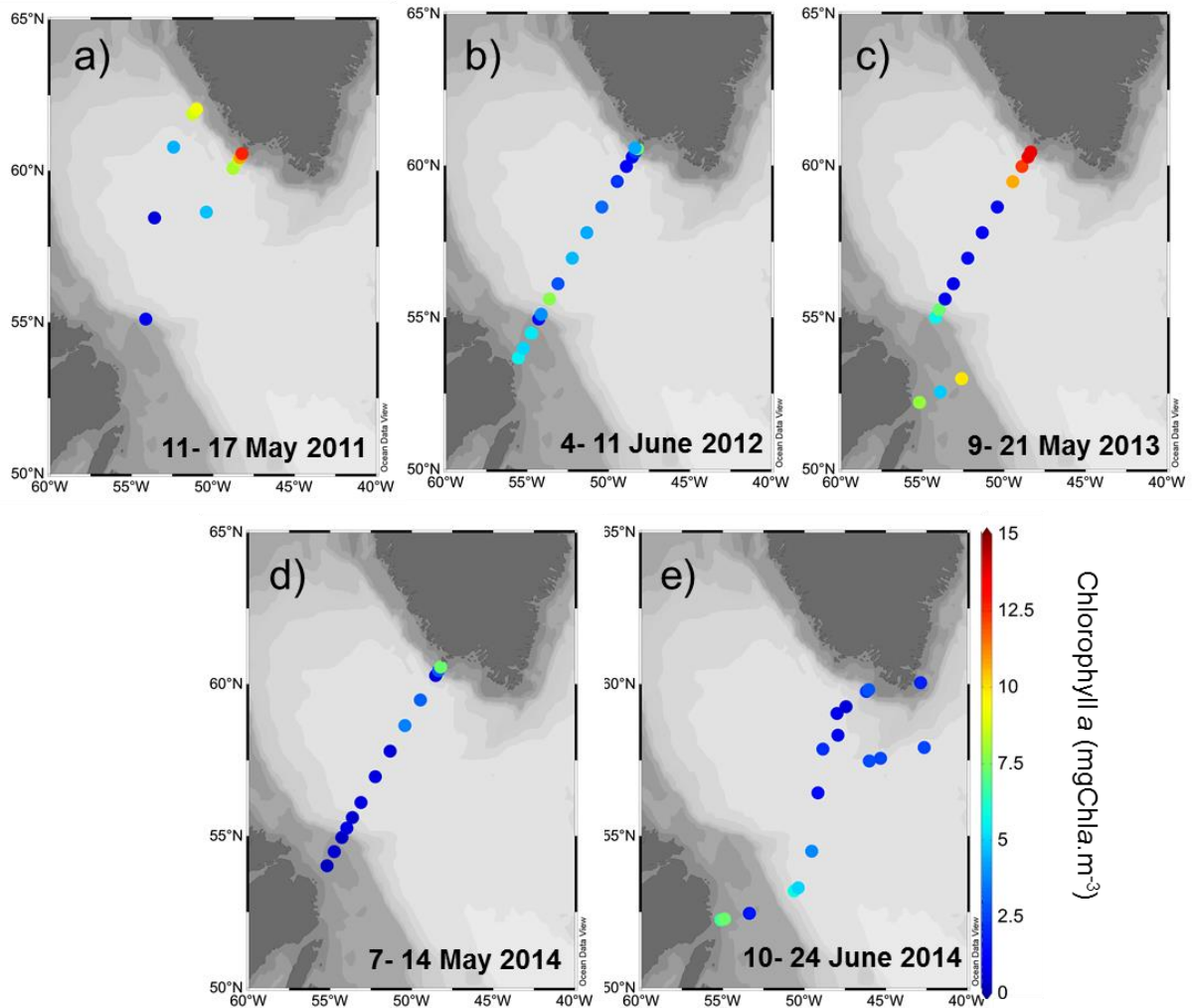
389

390 Figure 3. Boxplots (median, upper and lower quartile, minimum and maximum values and
 391 outliers) of (a,b) silicate, (c,d) nitrate, (e,f) phosphate and (g,h) ammonium concentrations, in addition
 392 to (i,j) Si^* (silicate minus nitrate concentrations) from the upper 50 m and (k,l) from approximately
 393 200 m water depth in May (left) and June (right) among each biogeographical zone of the Labrador
 394 Sea: Labrador Shelf (LSh) + Labrador Slope (LSI), Central Basin (CB) and Greenland Slope (GSI) +
 395 Greenland Shelf (GSh).

396

397 *3.2 Chlorophyll a concentrations*

398 Chlorophyll *a* biomass was concentrated within subsurface waters (upper 50 m) of the
399 Labrador Sea (Figure 8 and 9, supplemental material). Thus, average concentrations of
400 chlorophyll (upper 50 m) were used to show the spatial variation of subsurface blooms across
401 the Labrador Sea. The chlorophyll *a* distribution (average of the upper 50 m) varied spatially
402 and interannually (Fig. 4). In general, the eastern Labrador Sea, near and within the
403 Greenland Slope and Shelf waters, had the highest subsurface (< 50 m) concentrations of
404 chlorophyll *a*, particularly during May 2011 and 2013 (Fig. 4a,c; average >10 mg chl*a* m⁻³).
405 The Labrador Shelf and Slope also had relatively high near surface chlorophyll *a* values (>5
406 mg chl*a* m⁻³) in all years, except during May 2014, possibly because sampling was before the
407 formation of the bloom (Fig. 4d). The offshore waters of the central Basin generally had
408 lower near surface chlorophyll *a* concentrations (<5 mg chl*a* m⁻³) than the shelves in May,
409 but later in the season (June 2012, 2014) average subsurface chlorophyll *a* values were ~ 5
410 mg chl*a* m⁻³ (Fig. 4b,e).



411

412 Figure 4. Chlorophyll *a* distribution (average of 0 – 50 m values) at each station of the Labrador Sea
 413 during late spring/early summer 2011 - 2014 (a-e). Cruise dates are given in each panel.

414

415 3.3 Phytoplankton community structure

416 Cluster analysis of phytoplankton biomass from the Labrador Sea during spring and
 417 summer of 2011 - 2014 distinguished seven major Clusters of samples with a similarity level
 418 of 46%. Non-metric multi-dimensional scaling (nMDS) analysis showed a two-dimensional
 419 spatial representation of the similarities within sampled stations based on the composition and
 420 biomass values (Fig. 5a). A stress level < 0.2 in the nMDS plot (Fig. 5a) corresponds to a
 421 ‘suitable’ two-dimensional representation of the similarity relationships of the samples within
 422 and between Clusters (as defined in Clarke, 1993). ANOSIM one-way analysis comparing

423 each Cluster suggested that they were significantly different in composition ($p = 0.001$, R
424 statistic from pairwise analysis varied from 0.75 – 1), and that the Cluster groups are well
425 separated, given that the R statistic values are approaching 1 (see Clarke and Warwick,
426 2001). Taxa whose cumulative contribution approximated 90% of the average similarity
427 within each Cluster are shown in Table 1.

428 Cluster 1 ($n = 12$) included the samples from the Labrador Shelf during June 2012 and
429 2014 and May of 2013 (Fig. 5c, d, f). This Cluster had the second highest average biomass
430 ($275 \pm 131 \text{ mg C m}^{-3}$) compared to the other Clusters identified, with large contributions to
431 the Group similarity from Arctic and sea-ice diatoms, such as *Thalassiosira* spp. (particularly
432 *T. hyalina*), *Porosira glacialis*, *Fragilariopsis* spp. (particularly *F. cylindrus* and *F.*
433 *oceanica*), *Fossula arctica*, *Bacterosira bathyomphala*, *Chaetoceros* spp. (e.g. *C. socialis* and
434 *Phaeoceros*) (Table 1) and *Coscinodiscus centralis*, in addition to unidentified small
435 dinoflagellates ($< 30 \mu\text{m}$), *Gyrodinium* spp., *Protoperidinium* and cryptophytes (Table 1).

436 Cluster 2 ($n = 10$) contained samples with relatively high biomass (average of $169 \pm$
437 105 mg C m^{-3}) compared with Clusters 3, 6 and 7 but lower than Clusters 1, 4 and 5. These
438 samples were from offshore waters of the centre of the Labrador Sea during June (early
439 summer - 2012, 2014) (Fig. 5c,f). Sub-arctic North Atlantic diatoms, such as *Ephemera*
440 *planamembranacea*, and *Fragilariopsis atlantica*, in addition to *Thalassiosira* spp. and
441 dinoflagellates (unidentified small and large armored, *Gyrodinium* spp.) all contributed to the
442 similarity of these samples (Table 1).

443 Dinoflagellates (unidentified small and *Gyrodinium* sp.), cryptophytes,
444 silicoflagellates (*Dictyocha speculum*) and the diatom *Pseudo-nitzschia* spp. contributed to
445 the similarity of samples in Cluster 3 ($n = 12$) (Table 1). These samples had the lowest

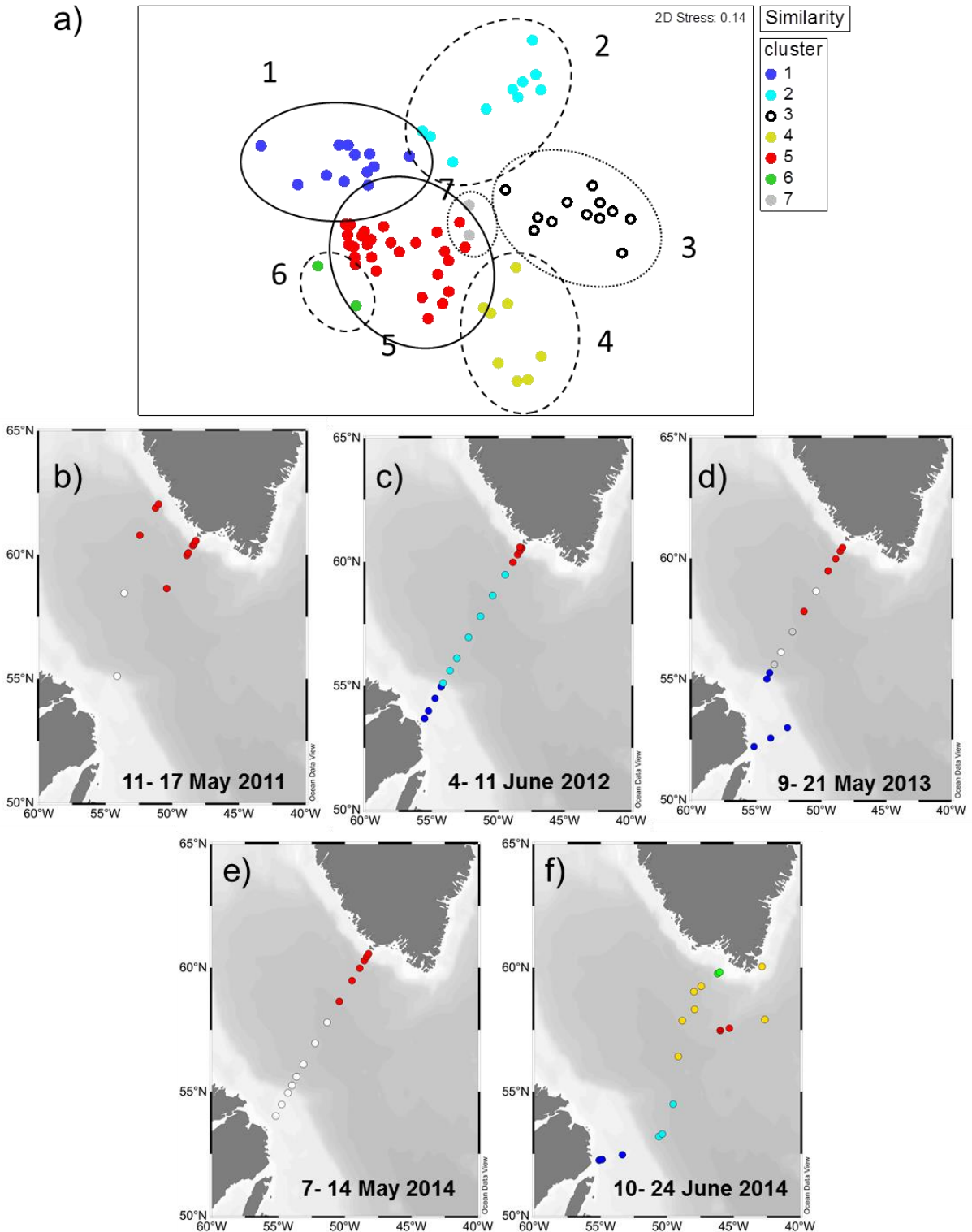
446 average biomass overall ($5 \pm 4 \text{ mg C m}^{-3}$) and came from the western-central region of the
447 Labrador Sea during May 2011, 2013, 2014 (late spring) (Table 1, Fig. 5b,d,e).

448 Cluster 4 ($n = 8$) included samples with the highest biomass overall (average = $304 \pm$
449 282 mg C m^{-3}) where the diatom *Rhizosolenia hebetata f. semispina* was the major
450 contributor to the similarity between samples (64%) (Table 1). Other diatoms, including
451 medium to large *Chaetoceros* spp. (e.g. *C. decipiens* and *Phaeoceros*) and *Pseudo-nitzschia*
452 *granii*, dinoflagellates (unidentified naked), cryptophytes and the prymnesiophyte
453 *Phaeocystis pouchetii* contributed up to almost 90% of the cumulative similarity (Table 1).
454 Samples from this Cluster occurred only in the central region of the Labrador Sea and later in
455 the season (mid-summer; late June) during 2014 (Fig. 5f).

456 The prymnesiophyte *Phaeocystis pouchetii* was the major contributor to samples in
457 Cluster 5 ($n = 28$), with the third highest average biomass ($248 \pm 181 \text{ mg C m}^{-3}$) (Table 1).
458 Diatoms such as *Thalassiosira* spp., *Rhizosolenia hebetata f. semispina*, *Pseudo-nitzschia*
459 *granii*, *Porosira glacialis* and *Chaetoceros* (*Phaeoceros*, but mostly *C. socialis*), in addition
460 to dinoflagellates (small unidentified and *Gyrodinium* spp.) also contributed cumulatively to
461 almost 90% of similarity of these samples (Table 1). Samples from Cluster 5 also had the
462 highest average chlorophyll *a* biomass (Table 2) and occurred in the central-eastern section of
463 the Labrador Sea (along and/or on the nearby Greenland shelf) during all years (2011 - 2014)
464 (Fig. 5b-f).

465 Cluster 6 ($n = 2$) comprised two samples from Greenland Shelf waters during summer
466 2014 (Fig. 5f), with relatively low biomass ($87 \pm 14 \text{ mg C m}^{-3}$) (Table 1). Small (e.g. *C.*
467 *socialis*) and medium-sized diatoms, such as *Chaetoceros* spp. (e.g. *C. decipiens*),
468 *Thalassiosira* spp. and *Rhizosolenia hebetata f. semispina*, in addition to the flagellate *P.*
469 *pouchetii* contributed up to 77% of the similarity for these samples (Table 1).

470 Cluster 7 (n = 2) stations also had relatively low average biomass ($33 \pm 4 \text{ mg C m}^{-3}$)
471 and was comprised of just two samples from the central Labrador Sea during May 2013
472 (Table 1, Fig. 5d). Samples from this Cluster represent a mixture of Clusters 3 and 5, where
473 diatoms such as *Pseudo-nitzschia* spp., *Thalassiosira*, *Rhizosolenia hebetata f. semispina*,
474 *Corethron criophilum*, in addition to *P. pouchetii* and dinoflagellates (small unidentified
475 naked) contributed mostly to the similarity for these samples (Table 1).



476

477 Figure 5. Cluster analysis of phytoplankton community composition across the Labrador Sea and
 478 multiple years. (a) Non-metric Multi-dimensional scaling (nMDS) plot representing the similarity in
 479 phytoplankton community structure within sampled stations at 46% similarity level (outlines) based
 480 on carbon biomass values. Temporal aspects of the Clusters from communities observed during May
 481 and June (solid outline), May only (dotted outline) or June only (dashed outline) are revealed on the
 482 outlines that separates each Cluster. (b - f) Distribution maps of distinct Clusters represented in the
 483 nMDS plot at each station of the Labrador Sea during May and June of 2011 - 2014.

484

485 Table 1. Percentage contribution of each taxa to the similarity of sampled stations, cumulative
 486 contribution up to approximately 90% and average similarity and biomass within each cluster.
 487 Numbers in bold refer to taxa whose cumulative contribution were up to approximately 70%. See
 488 methods for size (small, medium, large) classification. NI.- non-identified genus/species.

Taxa	Cluster 1	Cluster 2	Cluster 3	Cluster 4	Cluster 5	Cluster 6	Cluster 7
Armored dinoflagellates NI	2.6	5.8	13.1				2.8
<i>Bacterosira bathyomphala</i>	2.4						
<i>Chaetoceros</i> spp. (medium)				1.9		11.5	
<i>Chaetoceros</i> spp. (small)	1.4				2.7	30.6	
<i>Corethron criophilum</i>							7.4
<i>Coscinodiscus centralis</i>	1.1						
Cryptophytes	1.5		22.8	2.9			5.5
<i>Dictyocha speculum</i>			1.9				
<i>Ephemera planamembranaceae</i>		49.5					2.1
<i>Eucampia groelandica</i>							3.8
<i>Fossula arctica</i>	3.7						
<i>Fragilariopsis atlantica</i>		4.8					
<i>Fragilariopsis</i> spp. (large)	3.6						2.2
<i>Fragilariopsis</i> spp. (medium)	6.1					3.4	2.9
<i>Fragilariopsis</i> spp. (small)	3						1.6
<i>Gyrodinium</i> spp.	2.1	4.9	7		1.9	2.9	
Naked dinoflagellate NI (large)		3.6	4.5				2.3
Naked dinoflagellates NI (small)	5.2	12	32	8.7	4.9		10
<i>Nitzschia</i> spp.							1.6
<i>Phaeoceros</i> spp.	1.9			6.8	2.2		2.3
<i>Phaeocystis pouchetii</i>				4.7	42	6.9	6.5
<i>Porosira glacialis</i>	24.1				3	2.8	
<i>Protoperdinium</i> spp.	1.7	7.5				5.4	
<i>Pseudonitzschia granii</i>				2.6	3.3		2.5
<i>Pseudo-nitzschia</i> spp			1.9				14.3
<i>Rhisozolenia hebetata</i> f.				64.2	3.3	9	10.1
<i>Thalassiosira</i> spp.	30.1	5.2	8.4		27.1	19.2	13.9
Cumulative contribution (%)	90.3	93.4	91.5	91.7	90.3	91.7	91.6
Average similarity	59.7	60.1	56.2	62.8	57.1	74.4	79.7
Average biomass (mgC.m ⁻³)	275±13	169±10	5±4	304±28	248±18	87±14	33±4

489

490

491 *3.4 Hydrographic influence on phytoplankton community structure*

492 Hydrographic variables that explained the variance (explanatory variables) in the
 493 biomass of selected phytoplankton taxa (biomass greater than 0.5% of total) were
 494 investigated using redundancy analysis (RDA). The ordination diagram (Fig. 6) revealed
 495 associations between each taxon and the explanatory variables. Proximity of taxa to the
 496 environmental variables (arrows) in the same or opposite direction suggests positive or
 497 negative correlations, whereas no proximity indicates weak or a lack of correlation; the

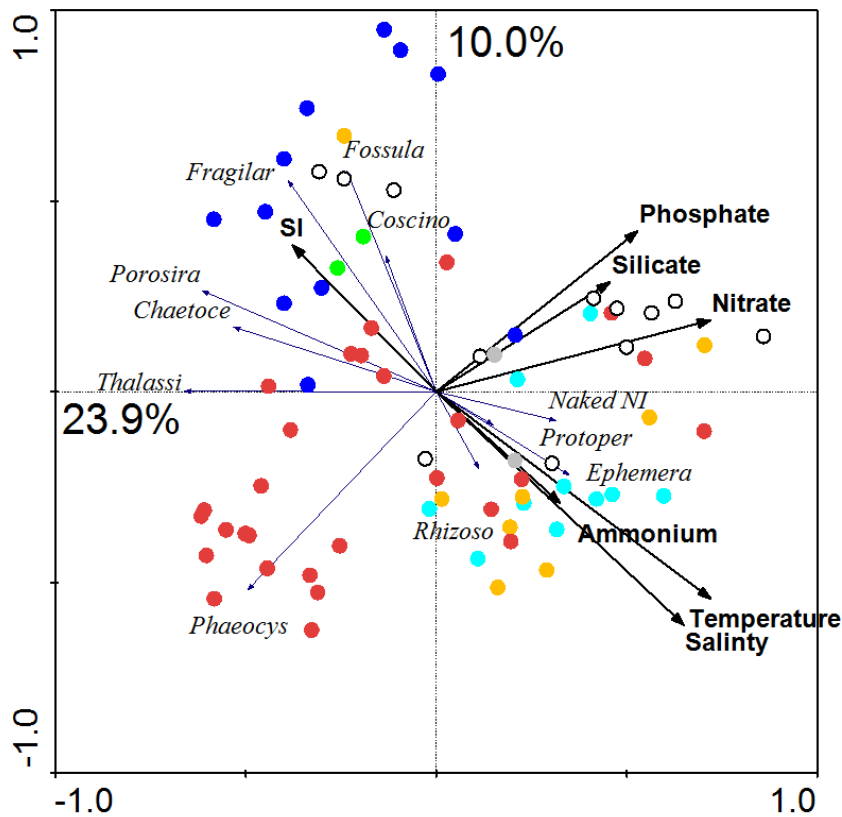
498 longer the arrow, the stronger the correlation. The associations in the ordination diagram
499 show that Arctic diatoms (Cluster 1, such as *Fossula arctica*, *Coscinodiscus*, *Fragilariopsis*
500 spp., *Porosira glacialis* and *Thalassiosira* spp., in addition to *Chaetoceros* spp., particularly
501 *C. socialis* - Cluster 6) occurred in colder (median temperature < 0°C), fresher (median
502 salinity < 33.0) and more stratified waters (median SI > 14 x 10³ kg m⁻⁴) (Table 2).

503 *Phaeocystis pouchetii* (Cluster 5) dominated in waters where nutrient concentrations
504 (mainly nitrate, but also phosphate and silicate) were low (median nitrate concentration < 3.7
505 µM) (Table 2). *Ephemera planamembranaceae* (Cluster 2) and *Rhizosolenia hebetata* f.
506 *semispina* (Cluster 4) were found in relatively warmer waters (median > 4.7°C) with higher
507 salinities (median > 34.5). Dinoflagellates (unidentified small and *Protoperidinium*,
508 Clusters 3 and 7) were common in less stratified waters (median SI = 0.1 x 10³ kg m⁻⁴) and
509 higher nitrate (median > 9 µM), phosphate (median > 0.7 µM) and silicate (median > 4.5 µM)
510 concentrations (i.e. pre-bloom conditions) (Fig. 6, Table 2).

511 The first axis (x- axis) of the analysis explained most of the variance (eigen-value =
512 23.9%, cumulative percentage variance between taxa and environmental factors = 58.0%),
513 whereas all canonical axes explained 98.3% of the variance (axis 1, p = 0.001; all axes, p =
514 0.001) (Fig. 6, Table 3). This means that (1) the arrows displayed closer to the x-axis
515 explained most of the variability in the data, and that (2) environmental variables explained
516 almost 100% of the variation of the selected taxa, when all four axes were analysed together.

517 Forward selection showed that of all seven environmental factors (Table 3) included
518 in the analysis, only four (temperature, nitrate, salinity and phosphate) best explained the
519 variance in the phytoplankton taxa biomass when analysed together. When all the forward-
520 selected variables were analysed together (conditional effects, referred to as λ_a in Table 3),
521 temperature was the most significant explanatory variable ($\lambda_a = 0.16$, p = 0.001), followed by

522 nitrate concentration and salinity ($\lambda_a = 0.1$, $p = 0.001$) (Table 3). Phosphate concentration was
 523 also a significant explanatory variable ($\lambda_a = 0.03$, $p = 0.048$) (Table 3). Although not
 524 significantly ($p < 0.05$) different ($\lambda_a = 0.01$, $p = 0.094$), silicate concentrations also had a
 525 slight influence as an explanatory variable (Table 3). Ammonium concentration and SI were
 526 not significant explanatory variables in this study.



527

528 Figure 6. Ordination diagram generated from redundancy analysis (RDA). Triplot represents taxa
 529 carbon biomass (thin lines), the significant explanatory variables (thick lines) and samples/stations
 530 (closed circles; colours refers to cluster groups on Figure 5a). Chaetoce = small *Chaetoceros* (mostly
 531 *C. socialis*), Coscino= *Coscinodiscus centralis*, Ephemera = *Ephemera planamembranaceae*, Fossula
 532 = *Fossula arctica*, Fragilar = *Fragilariopsis* medium (mostly *F. cylindrus*), Naked NI = Small (< 30
 533 μm) naked unidentified dinoflagellates, Phaeocys = *Phaeocystis pouchetii*, Porosira = *Porosira*.
 534 *glacialis*, Protoper = *Protoperidinium* spp., Rhizoso = *Rhizosolenia* spp., Thalassi = *Thalassiosira*
 535 spp. SI= Stratification Index.

536

537

538

539

540 Table 2. Median and standard error of hydrographic and biological parameters of each cluster. MLD=
 541 Mixed layer depth, SI= Stratification index.

Parameters	Cluster 1	Cluster 2	Cluster 3	Cluster 4	Cluster 5	Cluster 6	Cluster 7
$\sigma\theta$ (kg.m ⁻³)	26.2 ± 0.1	27.3 ± 0	27.6 ± 0.2	27.4 ± 0.2	27.1 ± 0.1	25.8 ± 0	27.5 ± 0.1
Salinity	32.6 ± 0.1	34.6 ± 0.1	34.8 ± 0.2	34.6 ± 0.4	33.9 ± 0.1	32.1 ± 0.1	34.6 ± 0.1
Temperature (°C)	-0.3 ± 0.2	4.8 ± 0.4	3.3 ± 0.6	4.9 ± 0.8	1.6 ± 0.3	-0.7 ± 0	3.3 ± 0
Silicate (µM)	4.3 ± 0.4	3.7 ± 0.3	7.6 ± 0.5	2.8 ± 0.6	3.5 ± 0.3	0.3 ± 0.1	4.7 ± 0.8
Phosphate (µM)	0.6 ± 0	0.5 ± 0.1	0.9 ± 0	0.4 ± 0.1	0.4 ± 0	0.2 ± 0	0.8 ± 0.1
Nitrate (µM)	3.8 ± 0.3	5.4 ± 0.7	13.4 ± 0.9	4.5 ± 1.2	3.6 ± 0.6	0.8 ± 0	9.9 ± 1.0
Si*	0.3 ± 0.1	-2.0 ± -0.6	-5.6 ± -1.6	-0.8 ± -0.3	-0.4 ± -0.1	-0.4 ± -0.3	-5.2 ± -3.7
Ammonia (µM)	0.4 ± 0.1	0.7 ± 0.1	0.5 ± 0.1	0.6 ± 0.3	0.6 ± 0.1	0	1.1 ± 0.1
MLD (m)	19.5 ± 1.4	20.0 ± 3.3	76.0 ± 89.5	24.0 ± 2.3	24.5 ± 4.9	15.0 ± 0	87.5 ± 3.5
C biomass (mgC.m ⁻³)	262 ± 38	147 ± 33	4.0 ± 1.0	251 ± 100	228 ± 34	87 ± 10	33 ± 3
Chlorophyll (mgchl _a .m ⁻³)	5.6 ± 0.7	4.0 ± 0.5	0.5 ± 0.1	1.4 ± 0.2	5.9 ± 0.8	2.5 ± 0.3	1.0 ± 0.2
Stratification Index	14.9 ± 4.8	6.6 ± 0.6	0.1 ± 0.4	7.4 ± 2.2	5.1 ± 1.2	16.0 ± 2.3	0.1 ± 0.01

542

543

545 Table 3. Variance explained by each explanatory variable (temperature (°C), nitrate, phosphate,
 546 silicate and ammonium (μM), salinity and SI (kg m^{-4})) when analysed alone (λ_1 , marginal effects) or
 547 when included in the model where other forward-selected variables are analysed together (λ_a ,
 548 conditional effects). Significant *p-values* (** $p < 0.05$) and ($*p < 0.1$) represents the variables that,
 549 together, significantly explain the variation in the analysis. SI= Stratification Index.

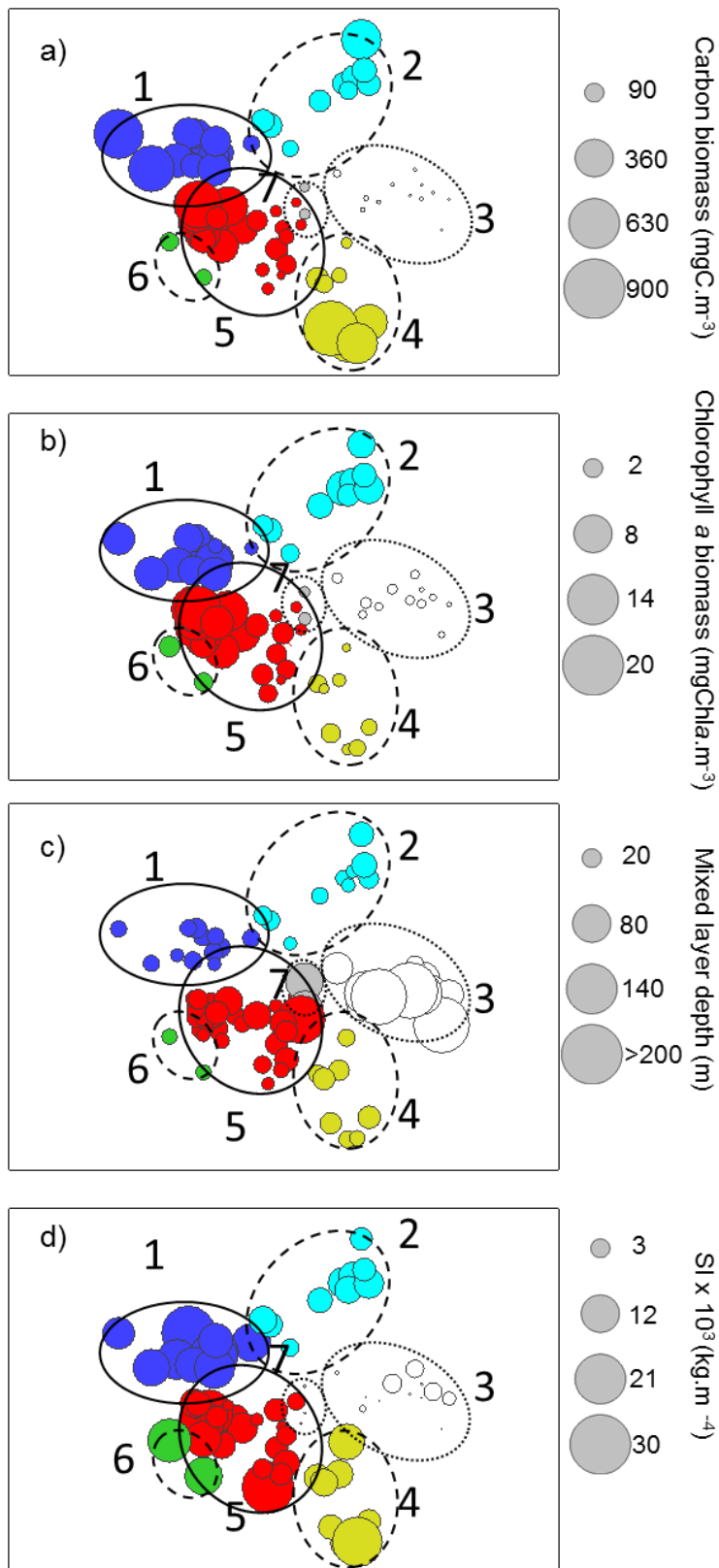
Marginal Effects		Conditional Effects				
Variable	λ_1	Variable	λ_a	<i>P</i>	<i>F</i>	
Temperature	0.16	Temperature	0.16	0.001*	13.37	
Nitrate	0.15	Nitrate	0.1	* 0.001*	9.72	
Salinity	0.14	Salinity	0.1	*	10.77	
Phosphate	0.11	Silicate	0.01	0.094* 0.043*	1.88	
Silicate	0.09	Phosphate	0.03	*	2.44	
SI	0.07	Ammonium	0.01	0.283	1.2	
Ammonium	0.04	SI	0	0.665	0.62	
Axes	1	2	3	4	Total variance	
Eigen-values	0.239	0.100	0.056	0.010	1	
Taxa-environment correlations	0.760	0.727	0.809	0.540		
Cumulative percentage variance						
of species data	23.9%	33.9%	39.5%	40.5%		
of species-environment relation	58.0%	82.3%	95.9%	98.3%		
Sum of all eigen-values					1	
Sum of all canonical eigen-values					0.412	
Test of significance of first canonical axis: eigen-value = 0.239; F-ratio = 20.702; P-value = 0.001 **						
Test of significance of all canonical axis: Trace = 0.412; F-ratio = 6.606; P-value = 0.001**						

550

551 3.5 Bloom development

552 To investigate the influence of hydrography on near surface (< 50 m) bloom
 553 development, MLD and SI were compared with Clusters that had a large biomass in terms of
 554 carbon and chlorophyll *a*. Five blooms (average chlorophyll *a* > 1.2 mg chl*a* m^{-3} per Cluster,
 555 see methods) belonged to Clusters 1, 2, 4, 5 and 6 and were composed of distinct
 556 phytoplankton communities observed in this study (Table 1). Shelf blooms, such as those
 557 located near or within Greenland Shelf waters (Clusters 5 and 6) and on the Labrador Shelf

558 (Cluster 1) had the highest biomass values, particularly Clusters 5 and 1 (median chl a = 5.9 \pm
559 0.8 mg chl a m $^{-3}$ and 5.6 \pm 0.7 mg chl a m $^{-3}$, respectively) (Table 2, Fig. 7a,b). Central Basin
560 blooms (Clusters 2 and 4) were weaker than shelf blooms (average values of chlorophyll a
561 concentration were 4.0 \pm 0.5 mg chl a m $^{-3}$ and 1.4 \pm 0.2 mg chl a m $^{-3}$, respectively) and
562 occurred later in the season (June) (Table 2, Fig. 7a,b). Stations with shallow mixed layers
563 (median < 25 m) and a higher stratification index (median SI > 5 x 10 3 kg m $^{-4}$) (Fig. 7c,d),
564 also had relatively high average biomass in terms of carbon and chlorophyll a (Fig. 7a,b,
565 Table 2). Low salinity waters (median < 33), found on the shelf (particularly Clusters 1 and
566 6) contributed to the shallow mixed layer depths (median < 20 m) and high stratification
567 levels observed (i.e. haline stratification, median SI > 14x 10 3 kg m $^{-4}$), whereas relatively
568 high sea surface temperature in June (> 4°C) in the central region of the Labrador Sea
569 induced stratification (median SI from 6.0 to 8.0 x 10 3 kg m $^{-4}$, Clusters 2 and 4) and shoaled
570 the mixed layer (i.e. thermal stratification, median mixed layer depths < 25 m) (Table 2).



571

572 Figure 7. Bubble plots derived from nMDS (see Figure 5a) representing the average values (upper 50
 573 m) of biomass in terms of (a) carbon, (b) chlorophyll *a*, (c) mixed layer depths (MLD), and (d)
 574 Stratification Index ($\text{SI} \times 10^{-3} \text{ kg m}^{-4}$) for the upper 60 m for each station. Filled colours refer to
 575 Cluster groups given in Figure 5a. Outlines around each Cluster represent the similarity in
 576 phytoplankton community structure within samples at 46% similarity level from samples collected
 577 during May and June (solid line), May only (dotted line) or June only (dashed line).

578

579 **4. Discussion**

580

581 *4.1 Influence of Arctic and Atlantic waters on phytoplankton species composition*

582 Phytoplankton community structure in the Labrador Sea during spring and early
583 summer (2011 - 2014) varied according to the hydrographic characteristics (temperature,
584 salinity and nutrient concentrations) of the distinct water masses of Atlantic (Irminger
585 Current and Subpolar Mode Water derived from the North Atlantic Current) and Arctic
586 (Labrador or West Greenland Current) origin, as well as their modifications at different
587 stages of transformation. Overall, Arctic/polar phytoplankton species were present in the
588 shelf waters, where the influence of Arctic waters was greater, whereas Atlantic
589 phytoplankton species dominated in the central Labrador Sea, with a greater contribution of
590 Atlantic water.

591 Blooms on the Labrador Shelf were comprised of Arctic and sea-ice diatoms that
592 were able to grow in cold (< 0°C) and relatively fresh waters (< 33) (Table 2). In our study,
593 polar/Arcto-boreal diatoms, such as *Thalassiosira* spp. (particularly *T. hyalina*, *T. antarctica*
594 *var. borealis*, *T. nordenskiöldii*, *T. gravida* and *T. constricta*, data not shown) and
595 *Bacterosira bathyomphala* were predominant in this region, which is consistent with the
596 strong Arctic water influence via the Labrador Current on the Labrador Shelf (von Quillfeldt,
597 2001, 2000; Degerlund and Eilertsen, 2009; Sergeeva et al., 2010). Local sea ice melting also
598 influenced the composition of diatoms in this region. The polar, cold water coastal diatom
599 *Porosira glacialis* (Pike et al., 2009), and the sea-ice associated *Fossula arctica* and
600 *Fragilariopsis* species (particularly *F. cylindrus* and *F. oceanica*; Caissie et al., 2010) were

601 abundant in both shelf regions, particularly on the Labrador Shelf, where sea ice melts during
602 spring.

603 Polar diatom species, including *Thalassiosira* spp. (particularly *T. gravida*, *T.*
604 *nordenskioldii*, *T. antarctica* var. *borealis* and *T. hyalina*), *P. glacialis* and *C. socialis*, in
605 addition to Atlantic species (*Rhizosolenia hebetata* f. *semispina*), were also observed on and
606 near the Greenland shelf, suggesting that these waters were a mixture of Arctic and Atlantic
607 origin - a characteristic typical of waters off the West Greenland Current (De Sève, 1999).
608 Nonetheless, phytoplankton community structure differed from the Labrador Shelf, as the
609 boreal prymnesiophyte *Phaeocystis pouchetii* was predominant in the eastern Labrador Sea
610 (on and nearby the Greenland Shelf) during all study years, but was rarely observed on the
611 Labrador Shelf. The reoccurring presence of *P. pouchetii* blooms in the central-eastern part of
612 the Labrador Sea during spring is well-documented (Head et al., 2000; Stuart et al., 2000;
613 Harrison et al., 2013; this study), suggesting that conditions in these waters are suitable for *P.*
614 *pouchetii* growth every year (discussed below). *Pseudo-nitzschia granii*, a small needle-
615 shaped diatom also observed in the eastern section of the Labrador Sea, had its distribution
616 tightly linked to *P. pouchetii*, whose colony colonization by the diatom species has been
617 previously reported in Norwegian waters (Hasle and Heimdal, 1998; Sazhin et al., 2007).
618 High abundances of *Chaetoceros socialis* (herein referred to as Cluster 6) could potentially
619 have followed blooms of *P. pouchetii* and diatoms on the west Greenland Shelf. *Chaetoceros*
620 *socialis* has frequently been found during the later stages of blooms in Arctic waters (e.g.
621 Baffin Bay, von Quillfeldt, 2000), where they can grow at relatively low nutrient
622 concentrations (particularly silicate) because of their small cell size (< 10 µm) and lightly
623 silicified cell walls (Booth et al., 2002).

624 The diatom *Ephemera planamembranaceae* was the most abundant species in
625 offshore blooms observed in the central and central-western part of the Labrador Sea during

626 June 2012 and 2014 (Fig. 5). This species, typically reported in high numbers in the North
627 Atlantic (Semina, 1997; Barnard et al., 2004), has been previously associated with shallow
628 mixed layers and relatively high nutrient concentrations (Yallop, 2001); similar to conditions
629 found in this study (Fig. 6, Table 2). *Fragilariopsis atlantica* co-dominated with *E.*
630 *planamembranacea* in the central Labrador Sea. Unlike *F. cylindrus* and *F. oceanica*, *F.*
631 *atlantica* is not found in sea-ice, being restricted to the water column and is mainly found in
632 the Northern Atlantic Ocean (Lundholm and Hasle, 2010). The centric diatom *Rhizosolenia*
633 *hebetata f. semispina*, also a representative North Atlantic diatom, formed blooms in the
634 central eastern portion of the Labrador Sea in the summer of 2014 (Fig. 5). High numbers of
635 *Rhizosolenia hebetata f. semispina* were found in association with large (subgenus
636 *Phaeoceros*, *Thalassiostrix longissima*) and medium-sized diatoms (eg. *Chaetoceros*
637 *decipiens*) in our study and have been previously observed in Norwegian waters (Hegseth and
638 Sundfjord, 2008).

639

640 4.2 Environmental controls on *Phaeocystis* versus diatoms

641 In our study, all phytoplankton blooms were found in shallow mixed layers (median
642 depth < 25 m) and stratified waters (median SI = $1 \times 10^3 \text{ kg m}^{-4}$) (Table 2). However, during
643 May 2014 a *P. pouchetii* bloom occurred in the eastern section of the Labrador Sea prior to
644 the development of other phytoplankton blooms in the region. These *P. pouchetii* blooms
645 were found in deeper mixed layers (~ 50 m) than in other years (data not shown). While low
646 irradiances are not required for *Phaeocystis* growth, given that it can also be found in shallow
647 mixed layers (Fragoso, 2009; Fragoso and Smith, 2012), the ability to grow under low light
648 levels may confer on this species an advantage compared to larger diatoms. *P. pouchetii*
649 blooms have also been reported to occur earlier in the season (April) due to the earlier haline-

650 driven stratification (Head et al., 2000; Frajka-Williams et al., 2009; Frajka-Williams and
651 Rhines, 2010), when light levels are lower than in May or June and the mixed layer is still
652 deep (< 100 m, Harrison et al., 2013).

653 Laboratory findings have also confirmed the ability of the southern ocean *Phaeocystis*
654 species (*P. antarctica*) to grow faster and increase their photosynthetic efficiency under
655 dynamic light intensities, typically found in deeper mixed layers (Kropuenske et al., 2009,
656 2010; Arrigo et al., 2010; Mills et al., 2010). Because of their ability to grow under variable
657 light, it is possible that *P. pouchetii* could grow and outcompete with diatoms while the
658 mixed layer depth shoals. As opposed to *P. pouchetii*, which is able to thrive under low light
659 intensities, sea-ice diatoms (such as *F. cylindrus*) invest heavily in photoprotective
660 mechanisms. This allows them to better adapt to higher light intensities, which are typically
661 found in shallow mixed layers (Kropuenske et al., 2009, 2010; Arrigo et al., 2010; Mills et
662 al., 2010) as well as late spring sea ice.

663 Nutrient resource competition has been suggested as one possible explanation for the
664 spatial segregation of *Phaeocystis pouchetii* and diatom blooms in the Labrador Sea
665 (Harrison and Li, 2008; Harrison et al., 2013) and elsewhere (Jiang et al., 2014). In our study,
666 cylinder or ribbon-shaped chain diatoms (i.e. *Thalassiosira* spp., *Bacterosira bathyomphala*
667 and *Fragilariopsis cylindrus*) dominated the Labrador Shelf waters. Such waters had only
668 slightly higher Si* values compared to the Greenland Shelf (Cluster 1 compared to Cluster 5,
669 see Table 2). Nonetheless, climatological studies show that the Labrador Shelf has a surplus
670 of silicate (silicate minus nitrate, Si* > 0) in the upper 150 m that decreases eastward, which
671 might explain the high number of diatoms in the west (Harrison et al., 2013). In this study, a
672 nitrate surplus of deep waters (~ 200 m) was evident across Labrador Sea shelves and basin
673 (negative Si*); however, the Labrador Shelf and Slope had a higher surplus of silicate in deep
674 waters compared to the central eastern section of the Labrador Sea (Fig. 3k,l). Hence, the

675 availability of silicate in waters of the Labrador Shelf might influence the dominance of
676 diatoms in this region as *P. pouchetii* does not require silicate, which could also be an
677 explanation for the east-west taxonomic segregation. Silicate depletion, however, is not a
678 necessary condition for *P. pouchetii* blooms, since it can co-dominate with diatoms when
679 silicate is not limiting. Jiang et al. (2014) argued that, under conditions where *P. pouchetii* is
680 dominant or co-dominant in a bloom, a sufficiently high pre-bloom concentration of nitrate (~
681 8 μM for the Massachusetts Bay) is needed (irrespective of the Si:N ratio). This would allow
682 more time for this species to grow, given that *Phaeocystis* grows slower than diatoms (Jiang
683 et al., 2014). Uptake rates of oxidised and reduced forms of nitrogen have also been
684 considered as an explanation for contrasting *Phaeocystis* and diatom-dominated blooms in
685 the North Sea, where *Phaeocystis* has been reported to have greater advantage due to
686 ammonium uptake compared with diatoms (Tungaraza et al., 2003). Ammonium
687 concentration was greater in the central-eastern part of the Labrador Sea in this study (Fig.
688 3h), particularly in the Greenland Shelf and Slope during June, which could also have
689 favoured the formation of *P. pouchetii* blooms in these waters.

690 *Phaeocystis* sp. colonies can control their buoyancy in the water column as a function
691 of light levels (positive buoyancy under light conditions, Wang and Tang, 2010), which could
692 also confer an advantage when accessing nutrients. In our study, *P. pouchetii* blooms on the
693 Greenland Shelf were concentrated in the subsurface and sometimes below the mixed layer,
694 being distributed within the upper 50 m, contrary to the diatom bloom on the Labrador Shelf
695 which was restricted to the upper mixed layer (< 25 m) (Fig 8 and 9, supplemental material).
696 Similar to the results presented here, *Phaeocystis pouchetii* blooms have also been reported to
697 be concentrated in subsurface waters around Greenland (Waniek et al., 2005; Frajka-
698 Williams and Rhines, 2010) and are capable of reaching deeper waters in the Fram Strait (>
699 75 m in Vogt et al., 2012b).

700 *Phaeocystis* colonies may also be able to proliferate because of their ability to escape
701 predation by size mismatch (Jakobsen and Tang, 2002; Tang, 2003), unpalatable and toxic
702 substances production (Aanesen et al., 1998; Dutz et al., 2005) and poor nutritional value of
703 their colony matrix (Tang et al., 2001). In the eastern region of the central Labrador Sea basin
704 and in the Greenland slope and shelf regions, the copepod *Calanus finmarchicus* is abundant
705 in May-July ($> 70,000 \text{ m}^{-2}$, 0-100 m, Head et al., 2003, 2013), where it dominates the
706 biomass and is the most important grazer. Reports in the literature are somewhat
707 contradictory as to whether *Phaeocystis* is a good food source for *Calanus* (see review by
708 Nejstgaard et al., 2007), but most studies have been carried out with copepods and
709 *Phaeocystis* from waters east of Greenland. In the northwest Atlantic, however, filtration
710 rates for a mixed-species *Calanus* population from the Newfoundland Shelf were ~ 2.5 lower
711 when they were feeding on natural seawater containing mainly *Phaeocystis* compared with
712 when they were feeding on seawater that had a similar overall chlorophyll *a* concentration but
713 contained a mixture of diatoms (Head and Harris, 1996).

714

715 *4.4 Mixed layer depth, vertical stability and bloom development*

716 Many studies of phytoplankton dynamics in the Labrador Sea have focused on how
717 physical factors control the onset of the spring phytoplankton bloom (Wu et al., 2008a;
718 Frajka-Williams et al., 2009; Frajka-Williams and Rhines, 2010; Lacour et al., 2015) . In our
719 study, spring blooms in the Labrador Sea, irrespective of the hydrographic zone, occurred
720 mostly in shallow mixed layers and areas of enhanced upper water column stratification,
721 which suggests that vertical stability plays an important role in bloom development and
722 maintenance. A similar observation was found by Wu et al. (2008a), who combined satellite-
723 derived chlorophyll and historical data in modelling studies to confirm that mixed layer depth

724 plays a critical role in initiating the spring bloom in the Labrador Sea. While blooms
725 occurring in and near the shelf regions were due to haline-driven stratification, thermal-
726 stratification promoted blooms offshore, in the central Labrador Sea, as has been previously
727 observed (Wu et al., 2008; Frajka-Williams et al., 2009; Head et al., 2013).

728 Blooms have been reported to occur earlier along the eastern margin of the central
729 basin, and/or on the Greenland shelf because of the relatively shallow winter mixed layer
730 depth driven by haline stratification compared to the deep central basin (Frajka-Williams et
731 al., 2009; Head et al., 2013). A more recent study using calculated mixed layer
732 Photosynthetically Active Radiation (PAR) from Argo-floats and satellite observations
733 showed that the mean PAR levels within the mixed layer ($\sim 2.5 \text{ mol photons m}^{-2} \text{ d}^{-1}$) is the
734 same during the initiation of the haline-driven bloom near the Greenland Shelf as it is in the
735 thermal driven bloom occurring in the central Labrador Sea, which starts one month later
736 (Lacour et al., 2015). Although mean PAR values were not measured *in situ* but estimated
737 from satellite and Argo-float observations, Lacour et al. (2015) concluded that increased light
738 availability, driven by either thermal or haline stratification, seems to be strongly linked to
739 bloom onset in the Labrador Sea. On the Labrador Shelf, shoaling of the mixed layer,
740 resulting from melting ice, has previously been established as a major trigger of diatom
741 blooms (Wu et al., 2007). However, in spite of a lack of sea ice on the Labrador shelf in May
742 2014, which could be an indication of sea ice melting, the mixed layer remained deep (~ 60
743 m), possibly due to strong winds.

744

745 **5- Conclusion**

746 In this study we have shown that phytoplankton community structure from the
747 Labrador Sea during spring and early summer of 2011 - 2014 varied according to the major

748 hydrographic features (temperature, salinity and nutrient concentrations) of distinct water
749 masses of Atlantic (Irminger Current), Arctic via Davis Strait (Labrador Current) or Arctic
750 via Denmark Strait (West Greenland Current) origin. In spite of interannual variations, which
751 in this study are difficult to assess because of the different sampling periods among years and
752 short duration of analysed records, phytoplankton community structure in the Labrador Sea
753 spring blooms had remarkably similar spatial and temporal patterns across the four years of
754 sampling. Arctic/polar large ($> 50 \mu\text{m}$) diatoms dominated the blooms in the inshore branch
755 of the LC, which were most influenced by Arctic and sea ice melt waters. *P. pouchetii* co-
756 dominated with diatoms (*Pseudo-nitzschia granii*, *Thalassiosira* spp.) at the interface of the
757 Arctic (WGC) and Atlantic (IC) waters. *Ephemera planamembranacea*, *Rhizosolenia*
758 *hebetata* f. *semispina* and *Fragilariopsis atlantica* were the main species found in offshore
759 waters of the central basin, which is strongly influenced by Atlantic waters. Lower salinities
760 and temperatures were associated with the Arctic/polar species found in the shelf waters with
761 higher influence of the Arctic outflow. Pre-bloom Si^* (Si^* from deeper waters), which were
762 comparatively higher on the Labrador Shelf and Slopes, might have influenced the taxonomic
763 segregation of polar diatoms dominating the west and *P. pouchetii* dominating the eastern
764 blooms. Nonetheless, the reason why *P. pouchetii* forms large blooms in the central-eastern
765 region of the Labrador Sea remains unclear.

766 In this study, shelf blooms occurred due to haline-driven stratification, whereas the
767 central basin bloom occurred later (June), when higher surface temperatures promoted
768 vertical stability. All blooms were found in shallow mixed layers ($< 40 \text{ m}$) and more stratified
769 waters, which confirms that vertical stability plays an important role in bloom development
770 across the Labrador Sea. However, *Phaeocystis pouchetii* blooms were found in May 2014,
771 when the mixed layer was deeper (median = 75 m). This confirms the ability of *P. pouchetii*

772 to grow in deeper mixing layers, whereas Arctic/sea-ice diatom blooms were only found in
773 shallower mixed layers (< 25 m).

774

775 **6- Acknowledgements**

776 We would like to thank Sinhue Torres-Valdes and Brian King (National Oceanography
777 Centre) for providing the nutrient and hydrographic data from JR302 cruise and Elaine
778 Mitchell (The Scottish Association for Marine Science) for guidance on Arctic phytoplankton
779 taxonomy. Many thanks to Jeff Anning and Glen Harrison (Bedford Institute of
780 Oceanography) for collecting the Lugols samples. The officers and crew of the *CCGS*
781 *Hudson* and *RSS James Clark Ross* and the support of technicians and scientists from all
782 cruises in analysing and providing the nutrient, chlorophyll and hydrographic data are also
783 acknowledged. We are grateful to three reviewers who offered useful suggestions to improve
784 the manuscript. G.M.F. was funded by a Brazilian PhD studentship, Science without Borders
785 (CNPq, 201449/2012-9). This research was also partially funded by UK Ocean Acidification,
786 a National Environment Research Council grant (NE/H017097/1) through an added value
787 award.

788

789 **7- References**

- 790 Aanesen, R.T., Eilertsen, H.C., Stabell, O.B., 1998. Light-induced toxic properties of the marine alga
791 *Phaeocystis pouchetii* towards cod larvae. *Aquat. Toxicol.* 40, 109–121.
- 792 Acevedo-Trejos, E., Brandt, G., Merico, A., Smith, S.L., 2013. Biogeographical patterns of
793 phytoplankton community size structure in the oceans. *Glob. Ecol. Biogeogr.* 22, 1060–1070.
794 doi:10.1111/geb.12071
- 795 Anisimov, O.A., Vaughan, D.G., Callaghan, T. V., Furgal, C., Marchant, H., Prowse, T.D., Vilhjálmsson,
796 H., Walsh, J.E., Fitzharris, B., Zealand, N.E.W., Canada, T.P., Uk, D.G.V., 2007. Polar Regions
797 (Arctic and Antarctic). *Clim. Chang.* 15, 653–685.

798 Ardyna, M., Babin, M., Gosselin, M., Devred, E., Rainville, L., Tremblay, J.-É., 2014. Recent Arctic
799 Ocean sea-ice loss triggers novel fall phytoplankton blooms. *Geophys. Res. Lett.* 41, 6207–6212.
800 doi:10.1002/2014GL061047

801 Arrigo, K.R., Mills, M.M., Kropuenske, L.R., Van Dijken, G.L., Alderkamp, A.C., Robinson, D.H., 2010.
802 Photophysiology in two major southern ocean phytoplankton taxa: Photosynthesis and growth
803 of *Phaeocystis antarctica* and *Fragilariopsis cylindrus* under different irradiance levels. *Integr.*
804 *Comp. Biol.* 50, 950–966. doi:10.1093/icb/icq021

805 Arrigo, K.R., van Dijken, G., Pabi, S., 2008. Impact of a shrinking Arctic ice cover on marine primary
806 production. *Geophys. Res. Lett.* 35, L19603. doi:10.1029/2008GL035028

807 Barnard, R., Batten, S.D., Beaugrand, G., Buckland, C., Conway, D.V.P., Edwards, M., Finlayson, J.,
808 Gregory, L.W., Halliday, N.C., John, A.W.G., Johns, D.G., Johnson, A.D., Jonas, T.D., Lindley, J.A.,
809 Nyman, J., Pritchard, P., Reid, P.C., Richardson, A.J., Saxby, R.E., Sidey, J., Smith, M.A., Stevens,
810 D.P., Taylor, C.M., Tranter, P.R.G., Walne, A.W., Wootton, M., Wotton, C.O.M., Wright, J.C.,
811 2004. Continuous plankton records: Plankton Atlas of the north Atlantic Ocean (1958-1999). II.
812 Biogeographical charts. *Mar. Ecol. Prog. Ser.* doi:10.3554/mepsr011

813 Bhatia, M.P., Kujawinski, E.B., Das, S.B., Breier, C.F., Henderson, P.B., Charette, M.A., 2013.
814 Greenland meltwater as a significant and potentially bioavailable source of iron to the ocean.
815 *Nat. Geosci.* 6, 274–278. doi:10.1038/ngeo1746

816 Booth, B.C., Larouche, P., Bélanger, S., Klein, B., Amiel, D., Mei, Z.P., 2002. Dynamics of *Chaetoceros*
817 *socialis* blooms in the North Water. *Deep. Res. Part II Top. Stud. Oceanogr.* 49, 5003–5025.
818 doi:10.1016/S0967-0645(02)00175-3

819 Brun, P., Vogt, M., Payne, M.R., Gruber, N., O'Brien, C.J., Buitenhuis, E.T., Le Quéré, C., Leblanc, K.,
820 Luo, Y.-W., 2015. Ecological niches of open ocean phytoplankton taxa. *Limnol. Oceanogr.* n/a–
821 n/a. doi:10.1002/lno.10074

822 Caissie, B.E., Brigham-Grette, J., Lawrence, K.T., Herbert, T.D., Cook, M.S., 2010. Last Glacial
823 Maximum to Holocene sea surface conditions at Umnak Plateau, Bering Sea, as inferred from
824 diatom, alkenone, and stable isotope records. *Paleoceanography.* doi:10.1029/2008PA001671

825 Clarke, K.R., 1993. Non-parametric multivariate analyses of changes in community structure. *Austr. J.*
826 *Ecol.* 18, 117–143. doi:10.1111/j.1442-9993.1993.tb00438.x

827 Clarke, K.R., Warwick, R.M., 2001. Change in marine communities: an approach to statistical analysis
828 and interpretation, 2nd Editio. ed. PRIMER-E, Plymouth.

829 Collos, Y., 2002. Determination of particulate carbon and nitrogen in coastal waters., in: Subba Rao
830 DV (Ed.), *Pelagic Ecology Methodology*. A. A. Balkema Publishers, Tokyo, pp. 333–341.

831 Cota, G.F., 2003. Bio-optical properties of the Labrador Sea. *J. Geophys. Res.*
832 doi:10.1029/2000JC000597

833 De Sève, M.A., 1999. Transfer function between surface sediment diatom assemblages and sea-
834 surface temperature and salinity of the Labrador Sea. *Mar. Micropaleontol.* 36, 249–267.
835 doi:10.1016/S0377-8398(99)00005-5

836 Degerlund, M., Eilertsen, H.C., 2010. Main species characteristics of phytoplankton spring blooms in
837 NE Atlantic and Arctic waters (68-80° N). *Estuaries and Coasts* 33, 242–269.
838 doi:10.1007/s12237-009-9167-7

839 DeGrandpre, M.D., Körtzinger, A., Send, U., Wallace, D.W.R., Bellerby, R.G.J., 2006. Uptake and
840 sequestration of atmospheric CO₂ in the Labrador Sea deep convection region. *Geophys. Res.*
841 *Lett.* 33, L21S03. doi:10.1029/2006GL026881

842 Dickson, B., Yashayaev, I., Meincke, J., Turrell, B., Dye, S., Holfort, J., 2002. Rapid freshening of the
843 deep North Atlantic Ocean over the past four decades. *Nature* 416, 832–837.
844 doi:10.1038/416832a

845 Dutz, J., Klein Breteler, W.C.M., Kramer, G., 2005. Inhibition of copepod feeding by exudates and
846 transparent exopolymer particles (TEP) derived from a *Phaeocystis globosa* dominated
847 phytoplankton community. *Harmful Algae* 4, 929–940.

848 Finkel, Z. V., Beardall, J., Flynn, K.J., Quigg, A., Rees, T.A. V., Raven, J.A., 2010. Phytoplankton in a
849 changing world: Cell size and elemental stoichiometry. J. Plankton Res.
850 doi:10.1093/plankt/fbp098

851 Fragoso, G.M., 2009. Hydrography and phytoplankton distribution in the Amundsen and Ross Seas.
852 College of William and Mary.

853 Fragoso, G.M., Smith, W.O., 2012. Influence of hydrography on phytoplankton distribution in the
854 Amundsen and Ross Seas, Antarctica. J. Mar. Syst. 89, 19–29.
855 doi:10.1016/j.jmarsys.2011.07.008

856 Frajka-Williams, E., Rhines, P.B., 2010. Physical controls and interannual variability of the Labrador
857 Sea spring phytoplankton bloom in distinct regions. Deep. Res. Part I Oceanogr. Res. Pap. 57,
858 541–552. doi:10.1016/j.dsr.2010.01.003

859 Frajka-Williams, E., Rhines, P.B., Eriksen, C.C., 2009. Physical controls and mesoscale variability in the
860 Labrador Sea spring phytoplankton bloom observed by Seaglider. Deep. Res. Part I Oceanogr.
861 Res. Pap. 56, 2144–2161. doi:10.1016/j.dsr.2009.07.008

862 Goes, J.I., Gomes, H.D.R., Chekalyuk, A.M., Carpenter, E.J., Montoya, J.P., Coles, V.J., Yager, P.L.,
863 Berelson, W.M., Capone, D.G., Foster, R. a., Steinberg, D.K., Subramaniam, A., Hafez, M. a.,
864 2014. Influence of the Amazon River discharge on the biogeography of phytoplankton
865 communities in the western tropical north Atlantic. Prog. Oceanogr. 120, 29–40.
866 doi:10.1016/j.pocean.2013.07.010

867 Hall, M.M., Torres, D.J., Yashayaev, I., 2013. Absolute velocity along the AR7W section in the
868 Labrador Sea. Deep. Res. Part I Oceanogr. Res. Pap. 72, 72–87. doi:10.1016/j.dsr.2012.11.005

869 Harrison, G.W., Yngve Børshheim, K., Li, W.K.W., Maillet, G.L., Pepin, P., Sakshaug, E., Skogen, M.D.,
870 Yeats, P.A., 2013. Phytoplankton production and growth regulation in the Subarctic North
871 Atlantic: A comparative study of the Labrador Sea-Labrador/Newfoundland shelves and
872 Barents/Norwegian/Greenland seas and shelves. Prog. Oceanogr. 114, 26–45.
873 doi:10.1016/j.pocean.2013.05.003

874 Harrison, W., Li, W., 2008. Phytoplankton growth and regulation in the Labrador Sea: light and
875 nutrient limitation. J. Northwest Atl. Fish. Sci. doi:10.2960/J.v39.m592

876 Hasle, G.R., Heimdal, B.R., 1998. The net phytoplankton in Kongsfjorden, Svalbard, July 1988, with
877 general remarks on species composition of Arctic phytoplankton. Polar Res. 17, 31–52.
878 doi:10.1111/j.1751-8369.1998.tb00257.x

879 Head, E.J.H., Harris, L.R., 1996. Chlorophyll destruction by *Calanus* spp. grazing on phytoplankton:
880 Kinetics, effects of ingestion rate and feeding history, and a mechanistic interpretation. Mar.
881 Ecol. Prog. Ser. 135, 223–235. doi:10.3354/meps135223

882 Head, E.J.H., Harris, L.R., Campbell, R.W., 2000. Investigations on the ecology of *Calanus* spp. in the
883 Labrador Sea. I. Relationship between the phytoplankton bloom and reproduction and
884 development of *Calanus finmarchicus* in spring. Mar. Ecol. Prog. Ser. 193, 53–73.
885 doi:10.3354/meps193053

886 Head, E.J.H., Harris, L.R., Yashayaev, I., 2003. Distributions of *Calanus* spp. and other
887 mesozooplankton in the Labrador Sea in relation to hydrography in spring and summer (1995-
888 2000). Prog. Oceanogr. doi:10.1016/S0079-6611(03)00111-3

889 Head, E.J.H., Melle, W., Pepin, P., Bagøien, E., Broms, C., 2013. On the ecology of *Calanus*
890 *finmarchicus* in the Subarctic North Atlantic: A comparison of population dynamics and
891 environmental conditions in areas of the Labrador Sea-Labrador/Newfoundland Shelf and
892 Norwegian Sea Atlantic and Coastal Waters. Prog. Oceanogr. 114, 46–63.
893 doi:10.1016/j.pocean.2013.05.004

894 Hegseth, E.N., Sundfjord, A., 2008. Intrusion and blooming of Atlantic phytoplankton species in the
895 high Arctic. J. Mar. Syst. 74, 108–119. doi:10.1016/j.jmarsys.2007.11.011

896 Henson, S. a., Dunne, J.P., Sarmiento, J.L., 2009. Decadal variability in North Atlantic phytoplankton
897 blooms. J. Geophys. Res. Ocean. 114, 1–11. doi:10.1029/2008JC005139

898 Holm-Hansen, O., Lorenzen, C.J., Holmes, R.W., Strickland, J.D.H., 1965. Fluorometric Determination
899 of Chlorophyll. ICES J. Mar. Sci. 30, 3–15. doi:10.1093/icesjms/30.1.3

900 Jakobsen, H.H., Tang, K.W., 2002. Effects of protozoan grazing on colony formation in *Phaeocystis*
901 *globosa* (Prymnesiophyceae) and the potential costs and benefits 27, 261–273.

902 Jiang, M., Borkman, D.G., Scott Libby, P., Townsend, D.W., Zhou, M., 2014. Nutrient input and the
903 competition between *Phaeocystis pouchetii* and diatoms in Massachusetts Bay spring bloom. J.
904 Mar. Syst. 134, 29–44. doi:10.1016/j.jmarsys.2014.02.011

905 Kahru, M., Brotas, V., Manzano-Sarabia, M., Mitchell, B.G., 2011. Are phytoplankton blooms
906 occurring earlier in the Arctic? Glob. Chang. Biol. 17, 1733–1739. doi:10.1111/j.1365-
907 2486.2010.02312.x

908 Kerouel, R., Aminot, a, 1997. Fluorometric determination of ammonia in sea and estuarine water by
909 direct segmented flow analysis. Mar. Chem. 57, 265–275.

910 Kieke, D., Yashayaev, I., 2015. Studies of Labrador Sea Water formation and variability in the
911 subpolar North Atlantic in the light of international partnership and collaboration. Prog.
912 Oceanogr. 132, 220–232. doi:10.1016/j.pocean.2014.12.010

913 Kropuenske, L.R., Mills, M.M., Van Dijken, G.L., Alderkamp, A.C., Mine Berg, G., Robinson, D.H.,
914 Welschmeyer, N.A., Arrigo, K.R., 2010. Strategies and rates of photoacclimation in two major
915 southern ocean phytoplankton taxa: *Phaeocystis antarctica* (haptophyta) and *Fragilariopsis*
916 *cylindrus* (bacillariophyceae). J. Phycol. 46, 1138–1151. doi:10.1111/j.1529-8817.2010.00922.x

917 Kropuenske, L.R., Mills, M.M., van Dijken, G.L., Bailey, S., Robinson, D.H., Welschmeyer, N.A., Arrigo,
918 K.R., 2009. Photophysiology in two major Southern Ocean phytoplankton taxa: Photoprotection
919 in *Phaeocystis antarctica* and *Fragilariopsis cylindrus*. Limnol. Oceanogr. 54, 1176–1196.
920 doi:10.4319/lo.2009.54.4.1176

921 Lacour, L., Claustre, H., Prieur, L., Ortenzio, F.D., 2015. Phytoplankton biomass cycles in the North
922 Atlantic subpolar gyre: A similar mechanism for two different blooms in the Labrador Sea
923 5403–5410. doi:10.1002/2015GL064540.Received

924 Lepš, J., Šmilauer, P., 2003. Multivariate analysis of ecological data using CANOCO. Cambridge
925 university press.

926 Litchman, E., Edwards, K.F., Klausmeier, C. a., Thomas, M.K., 2012. Phytoplankton niches, traits and
927 eco-evolutionary responses to global environmental change. Mar. Ecol. Prog. Ser. 470, 235–
928 248. doi:10.3354/meps09912

929 Lundholm, N., Hasle, G.R., 2010. *Fragilariopsis* (Bacillariophyceae) of the Northern Hemisphere –
930 morphology, taxonomy, phylogeny and distribution, with a description of *F. pacifica* sp. nov.
931 Phycologia. doi:10.2216/09-97.1

932 Martz, T.R., DeGrandpre, M.D., Strutton, P.G., McGillis, W.R., Drennan, W.M., 2009. Sea surface
933 pCO₂ and carbon export during the Labrador Sea spring-summer bloom: An in situ mass
934 balance approach. J. Geophys. Res. 114, C09008. doi:10.1029/2008JC005060

935 Mathot, S., Smith, W.O., Carlson, C.A., Garrison, D.L., Gowing, M.M., Vickers, C.L., 2000. Carbon
936 partitioning within *Phaeocystis antarctica* (prymnesiophyceae) colonies in the Ross sea,
937 Antarctica. J. Phycol. 36, 1049–1056. doi:10.1046/j.1529-8817.2000.99078.x

938 Medlin, L.K., Priddle, J., 1990. Polar marine diatoms. British Antarctic Survey, Cambridge.

939 Menden-Deuer, S., Lessard, E.J., 2000. Carbon to volume relationships for dinoflagellates, diatoms,
940 and other protist plankton. Limnol. Oceanogr. 45, 569–579. doi:10.4319/lo.2000.45.3.0569

941 Mills, M.M., Kropuenske, L.R., Van Dijken, G.L., Alderkamp, A.C., Berg, G.M., Robinson, D.H.,
942 Welschmeyer, N.A., Arrigo, K.R., 2010. Photophysiology in two southern ocean phytoplankton
943 taxa: Photosynthesis of *Phaeocystis antarctica* (prymnesiophyceae) and *Fragilariopsis cylindrus*
944 (bacillariophyceae) under simulated mixed-layer irradiance. J. Phycol. 46, 1114–1127.
945 doi:10.1111/j.1529-8817.2010.00923.x

946 Montagnes, D.J.S., Franklin, D.J., 2001. Effect of temperature on diatom volume, growth rate, and
947 carbon and nitrogen content: Reconsidering some paradigms. Limnol. Oceanogr. 46, 2008–
948 2018. doi:10.4319/lo.2001.46.8.2008

949 Montes-Hugo, M., Doney, S.C., Ducklow, H.W., Fraser, W., Martinson, D., Stammerjohn, S.E.,
950 Schofield, O., 2009. Recent Changes in Phytoplankton Western Antarctic Peninsula. *Science*
951 (80-). 323, 1470–1473.

952 Nejstgaard, J.C., Tang, K.W., Steinke, M., Dutz, J., Koski, M., Antajan, E., Long, J.D., 2007. Zooplankton
953 grazing on *Phaeocystis* : A quantitative review and future challenges. *Biogeochemistry* 83,
954 147–172. doi:10.1007/s10533-007-9098-y

955 Olenina, I., Hajdu, S., Edler, L., Andersson, A., Wasmund, N., Busch, S., Göbel, J., Gromisz, S., Huseby,
956 S., Huttunen, M., Jaanus, A., Kokkonen, P., Ledaine, I., Niemkiewicz, E., 2006. Biovolumes and
957 size-classes of phytoplankton in the Baltic Sea. *HELCOM Balt. Sea Environ. Proc.* No. 106.

958 Pabi, S., van Dijken, G.L., Arrigo, K.R., 2008. Primary production in the Arctic Ocean, 1998–2006. *J.*
959 *Geophys. Res.* 113, C08005. doi:10.1029/2007JC004578

960 Peterson, T.D., Toews, H.N.J., Robinson, C.L.K., Harrison, P.J., 2007. Nutrient and phytoplankton
961 dynamics in the Queen Charlotte Islands (Canada) during the summer upwelling seasons of
962 2001–2002. *J. Plankton Res.* 29, 219–239. doi:10.1093/plankt/fbm010

963 Pike, J., Crosta, X., Maddison, E.J., Stickley, C.E., Denis, D., Barbara, L., Renssen, H., 2009.
964 Observations on the relationship between the Antarctic coastal diatoms *Thalassiosira*
965 *antarctica* Comber and *Porosira glacialis* (Grunow) Jørgensen and sea ice concentrations during
966 the late Quaternary. *Mar. Micropaleontol.* 73, 14–25. doi:10.1016/j.marmicro.2009.06.005

967 Rousseau, V., Mathot, S., Lancelot, C., 1990. Calculating carbon biomass of *Phaeocystis* sp. from
968 microscopic observations. *Mar. Biol.* 107, 305–314. doi:10.1007/BF01319830

969 Sazhin, A.F., Artigas, L.F., Nejstgaard, J.C., Frischer, M.E., 2007. The colonization of two *Phaeocystis*
970 species (Prymnesiophyceae) by pennate diatoms and other protists: A significant contribution
971 to colony biomass, in: *Phaeocystis* , Major Link in the Biogeochemical Cycling of Climate-
972 Relevant Elements. pp. 137–145. doi:10.1007/978-1-4020-6214-8_11

973 Semina, H.J., 1997. An outline of the geographical distribution of oceanic phytoplankton., in: Blaxter,
974 G.H.S., Southward, A.G., Gebruck, A.V., Southwards, E.C., Tyler, P.A. (Eds.), *Advances in Marine*
975 *Biology*. Academic Press, London, pp. 527–563. doi:10.1016/S0065-2881(08)60020-6

976 Sergeeva, V.M., Sukhanova, I.N., Flint, M. V., Pautova, L.A., Grebmeier, J.M., Cooper, L.W., 2010.
977 Phytoplankton community in the Western Arctic in July–August 2003. *Oceanology*.
978 doi:10.1134/S0001437010020049

979 Solórzano, L., 1969. Determination of ammonia in natural waters by the phenol hypochlorite
980 method. *Limnol. Oceanogr.* 14, 799–801. doi:10.4319/lo.1969.14.5.0799

981 Straneo, F., Saucier, F., 2008. The outflow from Hudson Strait and its contribution to the Labrador
982 Current. *Deep Sea Res. Part I Oceanogr. Res. Pap.* 55, 926–946. doi:10.1016/j.dsr.2008.03.012

983 Strutton, P.G., Martz, T.R., DeGrandpre, M.D., McGillis, W.R., Drennan, W.M., Boss, E., 2011. Bio-
984 optical observations of the 2004 Labrador Sea phytoplankton bloom. *J. Geophys. Res.* 116,
985 C11037. doi:10.1029/2010JC006872

986 Stuart, V., Sathyendranath, S., Head, E.J.H., Platt, T., Irwin, B., Maass, H., 2000. Bio-optical
987 characteristics of diatom and prymnesiophyte populations in the Labrador Sea. *Mar. Ecol. Prog.*
988 *Ser.* 201, 91–106. doi:10.3354/meps201091

989 Sun, J., Liu, D., 2003. Geometric models for calculating cell biovolume and surface area for
990 phytoplankton. *J. Plankton Res.* 25, 1331–1346. doi:10.1093/plankt/fbg096

991 Tang, K.W., 2003. Grazing and colony size development in *Phaeocystis globosa* (Prymnesiophyceae):
992 the role of a chemical signal. *J. Plankton Res.* 25, 831–842.

993 Tang, K.W., Jakobsen, H.H., Visser, a. W., 2001. *Phaeocystis globosa* (Prymnesiophyceae) and the
994 planktonic food web: Feeding, growth, and trophic interactions among grazers. *Limnol.*
995 *Oceanogr.* 46, 1860–1870. doi:10.4319/lo.2001.46.8.1860

996 Throndsen, J., Hasle, G.R., Tangen, K., 2007. *Phytoplankton of Norwegian coastal waters*. Almat
997 Forlag AS.

998 Tian, R.C., Deibel, D., Rivkin, R.B., Vézina, A.F., 2004. Biogenic carbon and nitrogen export in a deep-
999 convection region: Simulations in the Labrador Sea. *Deep. Res. Part I Oceanogr. Res. Pap.* 51,
1000 413–437. doi:10.1016/j.dsr.2003.10.015

1001 Tomas, C.R., 1997. Identifying marine phytoplankton. Academic press.

1002 Tungaraza, C., Rousseau, V., Brion, N., Lancelot, C., Gichuki, J., Baeyens, W., Goeyens, L., 2003.
1003 Contrasting nitrogen uptake by diatom and *Phaeocystis*-dominated phytoplankton assemblages
1004 in the North Sea. *J. Exp. Mar. Bio. Ecol.* 292, 19–41. doi:10.1016/S0022-0981(03)00145-X

1005 Utermöhl, H., 1958. Improvement of the quantitative methods for phytoplankton. *Mitt. Int. Ver.*
1006 *Limnol.* 9, 1–38.

1007 Vogt, M., O'Brien, C., Peloquin, J., Schoemann, V., Breton, E., Estrada, M., Gibson, J., Karentz, D., Van
1008 Leeuwe, M.A., Stefels, J., Widdicombe, C., Peperzak, L., 2012. Global marine plankton
1009 functional type biomass distributions: *Phaeocystis* spp. *Earth Syst. Sci. Data* 4, 107–120.
1010 doi:10.5194/essd-4-107-2012

1011 Von Quillfeldt, C., 2000. Common diatom species in Arctic spring blooms: their distribution and
1012 abundance. *Bot. Mar.* 43, 499–516. doi:10.1515/BOT.2000.050

1013 Von Quillfeldt, C., 2001. Identification of some easily confused common diatom species in Arctic
1014 spring blooms. *Bot. Mar.* 44, 375–389. doi:10.1515/BOT.2001.048

1015 Wang, X., Tang, K.W., 2010. Buoyancy regulation in *Phaeocystis globosa* Scherffel colonies. *Open*
1016 *Mar. Biol. J.* 4, 115–121.

1017 Waniek, J., Holliday, N., Davidson, R., Brown, L., Henson, S., 2005. Freshwater control of onset and
1018 species composition of Greenland shelf spring bloom. *Mar. Ecol. Prog. Ser.* 288, 45–57.
1019 doi:10.3354/meps288045

1020 Weller, R.A., Plueddemann, A.J., 1996. Observations of the vertical structure of the oceanic
1021 boundary layer. *J. Geophys. Res.* doi:10.1029/96JC00206

1022 Wu, Y., Peterson, I.K., Tang, C.C.L., Platt, T., Sathyendranath, S., Fuentes-Yaco, C., 2007. The impact
1023 of sea ice on the initiation of the spring bloom on the Newfoundland and Labrador Shelves. *J.*
1024 *Plankton Res.* 29, 509–514. doi:10.1093/plankt/fbm035

1025 Wu, Y., Platt, T., Tang, C., Sathyendranath, S., 2008. Regional differences in the timing of the spring
1026 bloom in the Labrador Sea. *Mar. Ecol. Prog. Ser.* 355, 9–20. doi:10.3354/meps07233

1027 Wu, Y., Platt, T., Tang, C.C.L., Sathyendranath, S., Devred, E., Gu, S., 2008. A summer phytoplankton
1028 bloom triggered by high wind events in the Labrador Sea, July 2006. *Geophys. Res. Lett.* 35,
1029 L10606.

1030 Yallop, M.L., 2001. Distribution patterns and biomass estimates of diatoms and autotrophic
1031 dinoflagellates in the NE Atlantic during June and July 1996. *Deep. Res. Part II Top. Stud.*
1032 *Oceanogr.* 48, 825–844. doi:10.1016/S0967-0645(00)00099-0

1033 Yankovsky, A.E., Yashayaev, I., 2014. Surface buoyant plumes from melting icebergs in the Labrador
1034 Sea. *Deep. Res. Part I Oceanogr. Res. Pap.* 91, 1–9. doi:10.1016/j.dsr.2014.05.014

1035 Yashayaev, I., 2007. Hydrographic changes in the Labrador Sea, 1960-2005. *Prog. Oceanogr.* 73, 242–
1036 276. doi:10.1016/j.pocean.2007.04.015

1037 Yashayaev, I., Loder, J.W., 2009. Enhanced production of Labrador Sea Water in 2008. *Geophys. Res.*
1038 *Lett.* 36. doi:10.1029/2008GL036162

1039 Yashayaev, I., Seidov, D., 2015. The role of the Atlantic Water in multidecadal ocean variability in the
1040 Nordic and Barents Seas. *Prog. Oceanogr.* 132, 68–127. doi:10.1016/j.pocean.2014.11.009

1041 Yashayaev, I., Seidov, D., Demirov, E., 2015. A new collective view of oceanography of the Arctic and
1042 North Atlantic basins. *Prog. Oceanogr.* doi:10.1016/j.pocean.2014.12.012

1043 Yebra, L., Harris, R.P., Head, E.J.H., Yashayaev, I., Harris, L.R., Hirst, A.G., 2009. Mesoscale physical
1044 variability affects zooplankton production in the Labrador Sea. *Deep. Res. Part I Oceanogr. Res.*
1045 *Pap.* 56, 703–715. doi:10.1016/j.dsr.2008.11.008

1046

1047